Supplementary information

Ring-Opening Copolymerization of (Dihydro)levoglucosenone-Derived Spiro-Epoxides and Cyclic Anhydrides

Tianle Gao,[a, ‡] Hiroto Ayakawa,[b, ‡] Tatsuya Nishimura,[c] Ayano Yoshida,[b] Moeno Sugiyama,[b] Takuya Yamamoto,[a] Kenji Tajima,[a] Kenji Takahashi,[d] Feng Li,[*a] Takuya Isono,[a] Katsuhiro Maeda,[e] Toshifumi Satoh[*a, f, g]

[a] Division of Applied Chemistry, Faculty of Engineering, Hokkaido University, Sapporo 060-8628, Japan;

[b] Graduate School of Chemical Sciences and Engineering, Hokkaido University, Sapporo 060-8628, Japan;

[c] Graduate School of Natural Science and Technology, Kanazawa University, Kakuma-machi, Kanazawa, 920-1192 Japan;

[d] Faculty of Biological Science and Technology, Institute of Science and Engineering, Kanazawa University, Kanazawa, 920-1192, Japan

[e] Nano Life Science Institute (WPI-NanoLSI), Kanazawa University, Kakuma-machi, Kanazawa, 920-1192 Japan;

[f] List Sustainable Digital Transformation Catalyst Collaboration Research Platform (ICReDD List-PF), Institute for Chemical Reaction Design and Discovery, Hokkaido University, Sapporo 001-0021, Japan;

[g] Department of Chemical & Materials Engi-neering, National Central University, Taoyuan 320317, Taiwan

Experimental Details.

Materials

Dihydrolevoglucosenone (Cyrene™; 99%, Sigma-Aldrich), trimethylsulfonium iodide (C_3H_9IS; >98.0%, TCI), trimethylsulfoxonium chloride (C_3H_9ClOS; 98%, Angene chemical), sodium hydride (NaH; 60%, dispersion in paraffin liquid, TCI), magnesium sulfate ($MgSO_4$; >98.0%, Kanto Chemical Co., Inc.), calcium hydride (CaH_2; >94%, Junsei Chemical Co., Ltd.), potassium trifluoroacetate (98%, Sigma-Aldrich), *trans*-2-[3-(4-*tert*-butylphenyl)-2-methyl-2-propenylidene]malononitrile (DCTB; >98.0%, TCI), phosphazene base *t*-BuP_1 (P_1-*t*-Bu; >97.0%, Sigma-Aldrich), phosphazene base *t*-BuP_2 (P_2-*t*-Bu; 2.0 M solution in THF, Sigma-Aldrich), Copper(I) iodide (CuI; 98.0%+, JUNSEI CHEMICAL CO., LTD.), 7-Methyl-1,5,7-triazabicyclo[4.4.0]dec-5-ene (MTBD; 98%, Sigma- Aldrich), and triethylborane (TEB; ca. 11% in Tetrahydrofuran, ca. 1mol/L, TCI), were used as received.

Phtalic anhydride (PA; >98%, TCI)、5-norbornene-*endo*-2,3-dicarboxylic anhydride (NA; 99%, Sigma-Aldrich)、glutaric anhydride (GA; >98%, TCI) were purified by sublimation, recrystallization using acetic anhydride, and subsequent sublimation prior to use. 1,4-Benzenedimethanol (BDM; >99.0%, TCI) was dried under high vacuum before use. Tetramethylammonium Acetate (TMAA; >98.0%, TCI) was dried under high vacuum at least 72 h prior to use. Cesium pivalate (CsOPiv; >97.0%, TCI) was dried by heating at 100°C under high vacuum for at least 72 h prior to use.

Instruments

The polymerization experiments were carried out in an MBRAUN stainless steel glovebox equipped with a gas purification system (molecular sieves and copper catalyst) in a dry argon atmosphere (H_2O, O_2 < 0.1 ppm). The moisture and oxygen contents in the glovebox were monitored by an MB-MO-SE 1 moisture sensor and an MB-OX-SE 1 oxygen sensor, respectively.

^{1}H and ^{13}C NMR measurements

The ^{1}H NMR (400 MHz) and ^{13}C NMR (100 MHz) spectra were recorded using a JEOL JNM-ECS 400 instrument at room temperature in $CDCl_3$.

Size exclusion chromatography (SEC)

The SEC using $CHCl_3$ as the eluent was performed at 40 °C (flow rate, 1.0 mL min^{-1}) using a Jasco high-performance liquid chromatography system (PU-4180 HPLC pump, AS-4550 auto sampler, and CO-4060 column oven) equipped with a Shodex K-800D guard column (8.0 mm × 100 mm; particle size, 10 μm), two Shodex columns (K-806L and K-804L; linear, 8.0 mm × 300 mm; particle size, 10 and 6 μm). The polystyrene standard curve ranging from 1,990 to 1,330,000 was used for calibration to achieve the molecular weight ($M_{n,\,SEC}$) and polydispersity index ($Đ$) of the polymers.

The SEC using THF as the eluent was performed at 40 °C (flow rate, 1.0 mL min^{-1}) using a Jasco high-performance liquid chromatography system (PU-4180 HPLC pump, AS-4550 auto sampler, and CO-2065 column oven) equipped with a Shodex KF-G 4A guard column (4.6 mm × 10 mm; particle size, 8 μm), two Shodex columns (KF-806L and KF-804L; linear, 8.0 mm × 300 mm; particle size, 10 and 7 μm). The polystyrene standard curve ranging from 1,990 to 1,330,000 was used for calibration to achieve the molecular weight ($M_{n,SEC}$) and polydispersity index ($Đ$) of the polymers.

Preparative SEC

The preparative SEC was performed at room temperature in $CHCl_3$ (flow rate, 10.0 mL min^{-1}) using LaboACE LC-7080 liquid chromatography system (Japan Analytical Industry Co. Ltd.) equipped with a P-LA80 pump, a RI-700LA RI detector, JAIGEL-HR-P guard column (8 mm × 40 mm; Japan Analytical Industry Co. Ltd.), JAIGEL-2HR column (linear, 20.0 mm × 600 mm; exclusion limit, 5.0 × 10^3) and JAIGEL-2.5HR column (linear, 20.0 mm × 600 mm; exclusion limit, 2.0 × 10^4).

Matrix-assisted laser desorption ionization time-of-flight mass spectrometry (MALDI-TOF MS)

The MALDI-TOF MS measurement of the obtained products was performed in reflector mode using a Bruker Daltonics (Germany) Ultraflex MALDI-TOF/TOF mass spectrometer equipped with a 355-nm Nd:YAG laser. A 1:1:1 (v/v/v) ratio of [**Polymer** (5 g L^{-1} in the corresponding solvent)]/[*trans*-2-[3-(4-*tert*-butylphenyl)-2-methyl-2-propenylidene]malononitrile (20 g L^{-1} in THF)]/[potassium trifluoroacetate (10 g L^{-1} in THF)] was used.

Differential scanning calorimetry (DSC) measurement

The DSC experiments were performed using a Hitachi DSC 7000X under a nitrogen atmosphere. The synthesized polyester samples were heated to 210 °C, cooled to −50 °C, and heated again to 280 °C at the 1st heating, cooling, and 2nd heating rate of 10 °C min^{-1}, 1 °C min^{-1} and 10 °C min^{-1}, respectively.

Thermogravimetric analysis (TGA) measurement

The TGA analysis was performed using Hitachi STA200RV under nitrogen atmosphere. The samples of polyesters were heated to 70 °C, cooled to 30 °C, and heated to 550 °C at the heating rate of 10 °C min^{-1}.

Electrospray ionization (ESI) Mass

High resolution mass spectrum of DBOOPh was measured with Thermo Scientific Exactive Plus Mass Spectrometer at the Instrumental Analysis and Open Facility Unit, Global Research Facility Alliance Center, Office for Integrated Technical Core Hub, Hokkaido University.

Powder X-ray diffraction (PXRD)

The PXRD measurement was performed using an X-ray diffractometer (SmartLab, Rigaku, rotating anticathode tube, 45 keV, 200 mA) with Ca Kα1 (λ = 0.154059 nm), a tube voltage and current of 45 keV and 200 mA, respectively, a step width of 0.01°, and speed of 4°/min.

Circular dichroism (CD) and Ultraviolet-Visible (UV–VIS) measurement

Circular dichroism (CD) spectra were recorded on a JASCO J-1500 circular dichroism spectrometer (JASCO, Japan) equipped with a Peltier-type temperature control unit. UV–VIS absorption spectra were measured using a JASCO V-750 UV–visible spectrophotometer equipped with a Peltier-type temperature control unit. Quartz cells with a path length of 1 mm were used for all measurements.Circular Dichroism and UV–vis Absorption.

Polymer samples were dissolved in chloroform or tetrahydrofuran (THF) to prepare solutions with concentrations of 10–12 mM (based on repeating units). The solutions were used without filtration. CD spectra were measured at −20 °C or 25 °C with a scanning speed of 50 nm min^{-1}, a response time of 2 s, and a bandwidth of 1 nm. Each spectrum represents the average of four scans, and the baseline of the corresponding solvent was subtracted. UV–vis absorption spectra were recorded at −20 °C using the same quartz cells (1 mm path length). The molar circular dichroism values (Δε) were calculated from the observed ellipticity using the concentration of repeating units.

Ring-opening alternating copolymerization (ROAC) of DBOO and cyclic anhydride

Scheme S1. ROAC of DBOO and PA

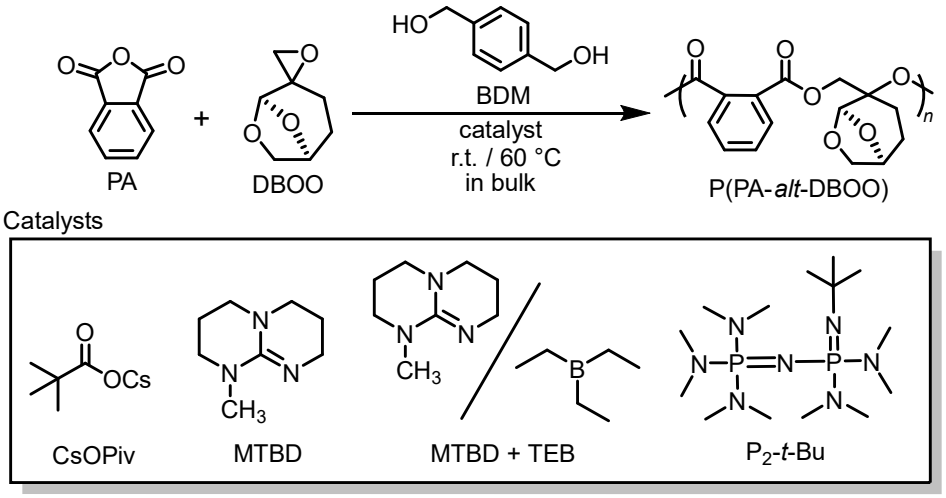

CsOPiv : cesium pivalate
MTBD : 7-methyl-1,5,7-triazabicyclo[4.4.0]dec-5-ene
TEB : triethylborane
P_2-*t*-Bu : phosphazene base *t*-BuP_2

A representative polymerization procedure using CsOPiv as the catalyst is described below.

Inside a dry glovebox, PA (1.51 g, 10.2 mmol, 70 eq.), $DBOO_{50:50}$ (4.11 g, 28.9 mmol, 200 eq.), 1,4-benzenedimethanol (BDM; 20.4 mg, 0.148 mmol, 1 eq.), and CsOPiv (350 mg, 0.150 mmol, 1 eq.) were charged into a flask equipped with a needle valve. The flask was removed from the glovebox and the reaction mixture was stirred at 60 °C for 20 h under an argon atmosphere. The polymerization was terminated by cooling to room temperature and adding CH_2Cl_2. The resulting crude product was reprecipitated in MeOH and subsequently purified by preparative SEC. Removal of the solvent under reduced pressure afforded P($DBOO_{50:50}$-*alt*-PA) as a yellowish-brown powder.

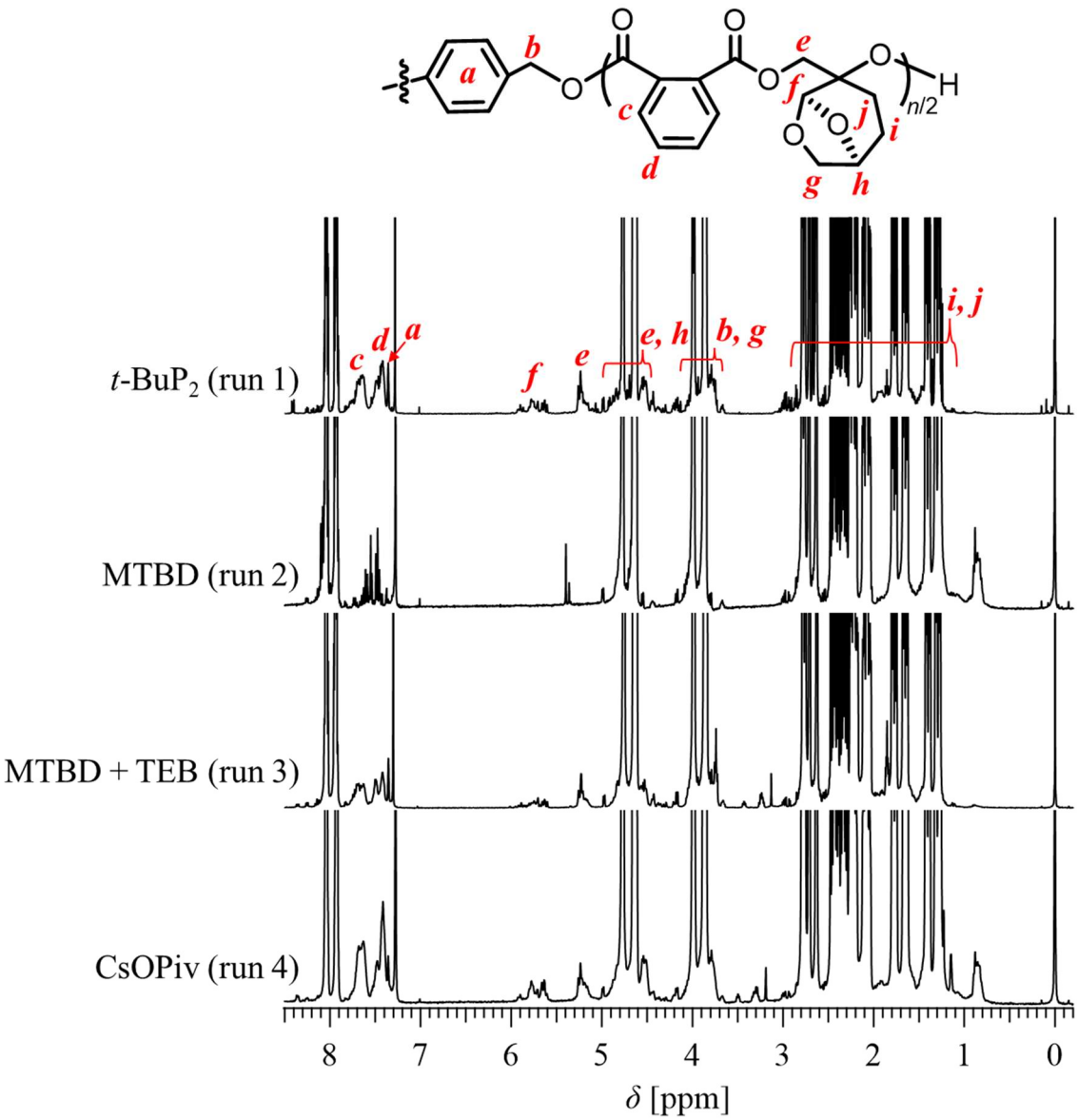

Figure S1. ^{1}H NMR spectrum of polymerization mixture before purification (runs 1-4 on Table 1).

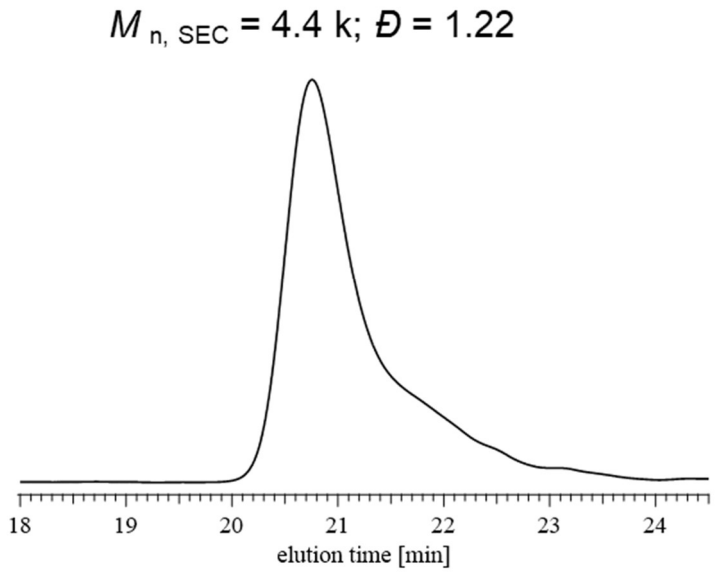

Figure S2. SEC trace of poly(DBOO$_{(50:50)}$-*alt*-PA) synthesized with CsOPiv (Table 1, run 5).

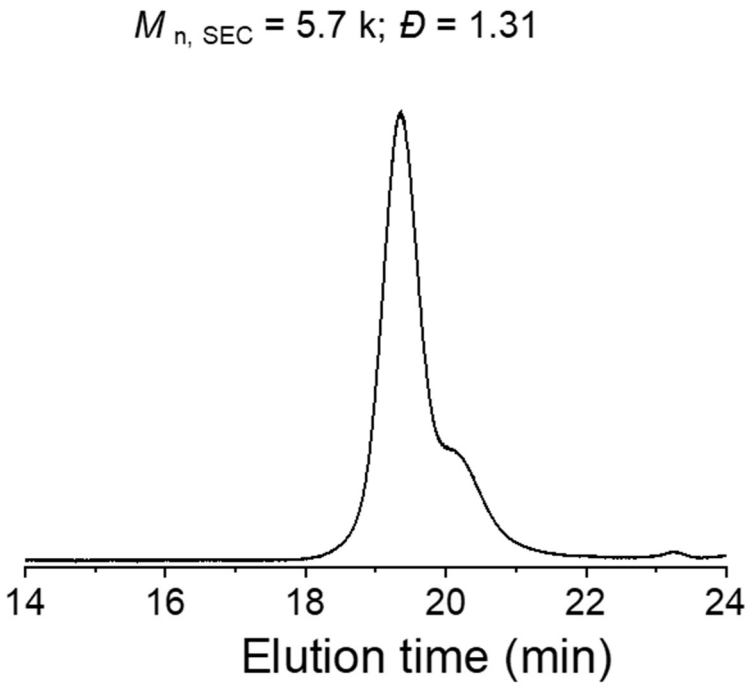

Figure S3. SEC trace of poly(DBOO$_{(87:13)}$-*alt*-PA) synthesized with CsOPiv (Table 1, run 9) measured in chloroform.

poly(DBOO$_{(87:13)}$-*alt*-PA)

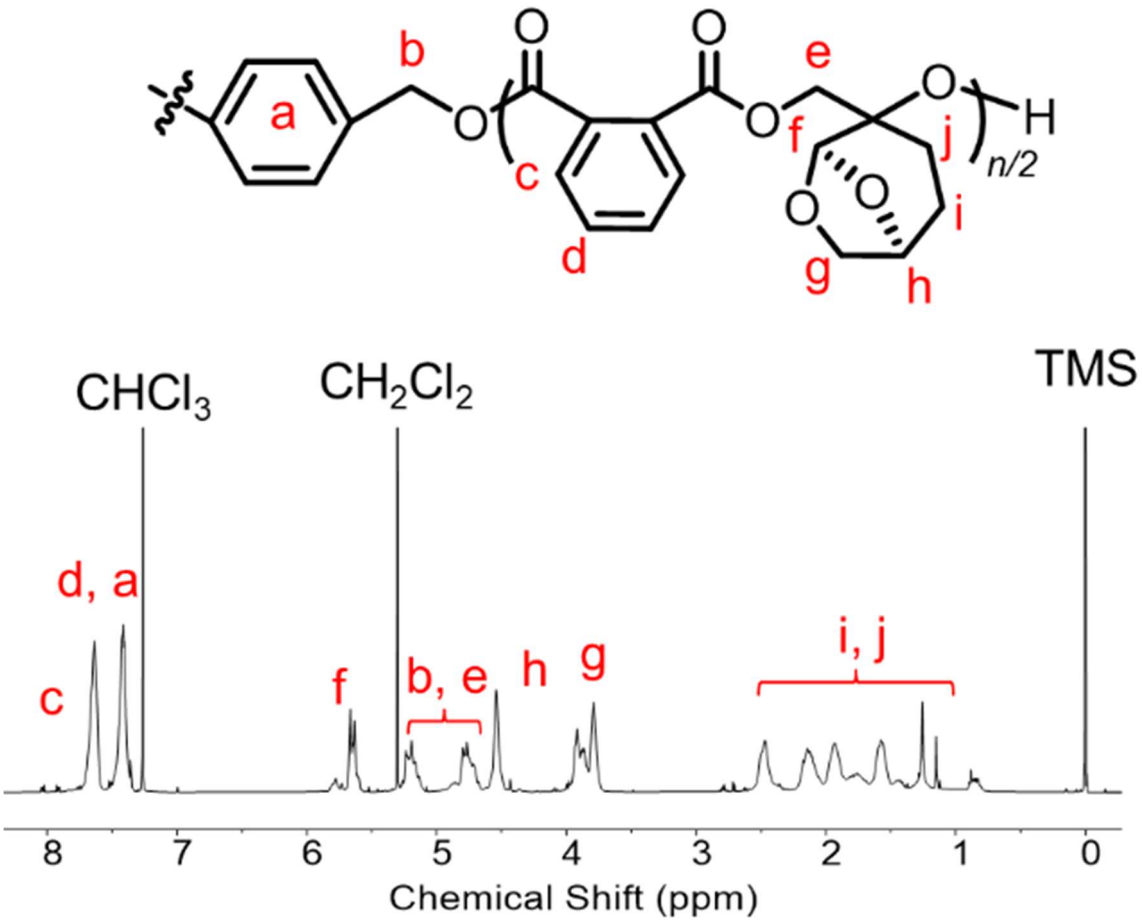

Figure S4. ^{1}H NMR spectrum and poly(DBOO$_{(87:13)}$-*alt*-PA) (Table 1, run 9; 400 MHz, $CDCl_3$).

poly(DBOO$_{(50:50)}$-*alt*-PA) VS. poly(DBOO$_{(87:13)}$-*alt*-PA)

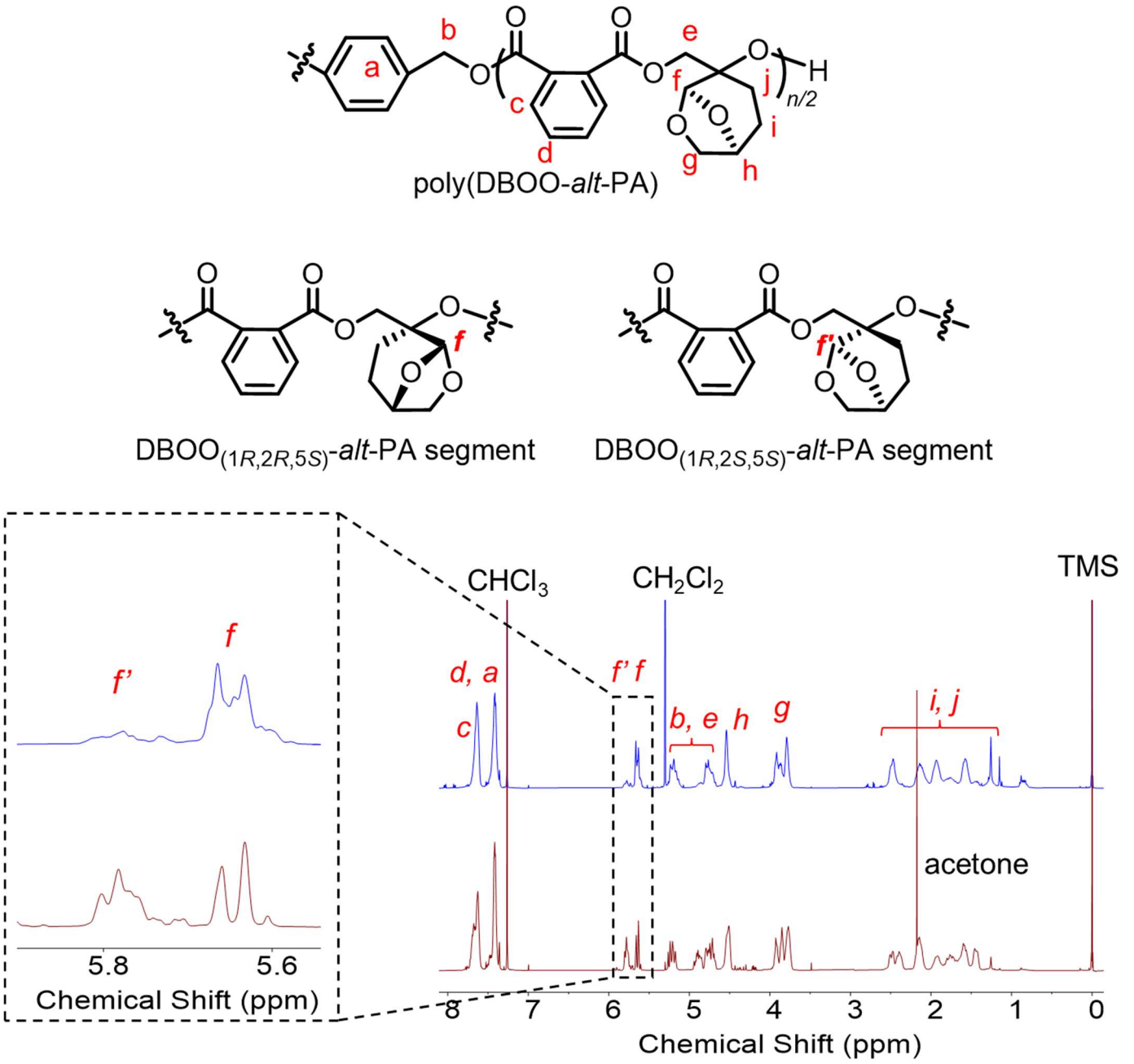

Figure S5. Comparison of ^{1}H NMR spectra of poly(DBOO$_{(50:50)}$-*alt*-PA) (down) and poly(DBOO$_{(87:13)}$-*alt*-PA) (upper)

Note: Although noticeable differences are observed in the signal patterns of these two polymers prepared from DBOO monomers with different dr values, it is difficult to make unambiguous assignments for the polymer segments derived from the different diastereomers. The most distinct difference appears in the signals corresponding to the acetal position (f and f'), for which a magnified view has been provided.

Table S1. Data for each sample at the time of sampling (according to **Figure 2D**)

Sampling number	Time (min)	Conv. $_{PA}$ (%)[a]	Conv. $_{DBOO}$ (%)[a]	Ratio of unreacted monomer		Conversion of diastereomeric	
				(1R,2S,5S)-DBOO (%)	(1R,2R,5S)-DBOO (%)	(1R,2S,5S)-DBOO (%)	(1R,2R,5S)-DBOO (%)
1	30	3.8	2.3	52.83	47.17	6.2 [b]	- [b]
2	60	10.0	6.2	54.55	45.45	6.9	5.2
3	120	12.1	11.5	52.43	47.57	15.7	6.5
4	250	23.8	21.2	53.8	46.2	22.9	19.1
5	360	29.8	26.9	51.85	48.15	31.1	21.8
6	540	42.5	39.6	52.17	47.83	42.7	35.8
7	780	58.5	56.5	52.68	47.32	58.4	54.3
8	960	71.1	68.8	50.98	49.02	71.1	66.1
9	1140	80.9	79.6	50.87	49.13	81.1	77.7

Polymerization conditions: Ar atmosphere; 100 ℃; n(BDM) =18.5 μmol; n(CsOPiv) = 18.5 μmol; n(PA) = 1.29 mmol, n(DBOO) = 1.29 mmol, Vol(toluene) = 258 μL; DBOO with a diastereomeric ratio of 55:45 was used.

[a] Determined by ^{1}H NMR spectrum of the obtained polymer in $CDCl_3$.

[b] The conversion data at 30 min of each DBOO diastereomer may contain large experiment error. They were not used in the plot (Figure 2D)

Note: The DBOO conversion data at 30 min could be an error. This data is not used in plot (**Figure 2D**).

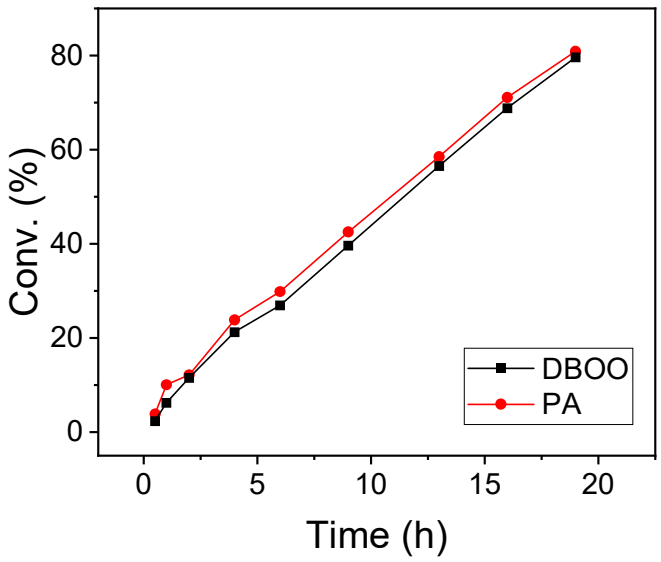

Figure S6. Monomer conversion monitoring during ROCOP of PA and DBOO (**Table S1**).

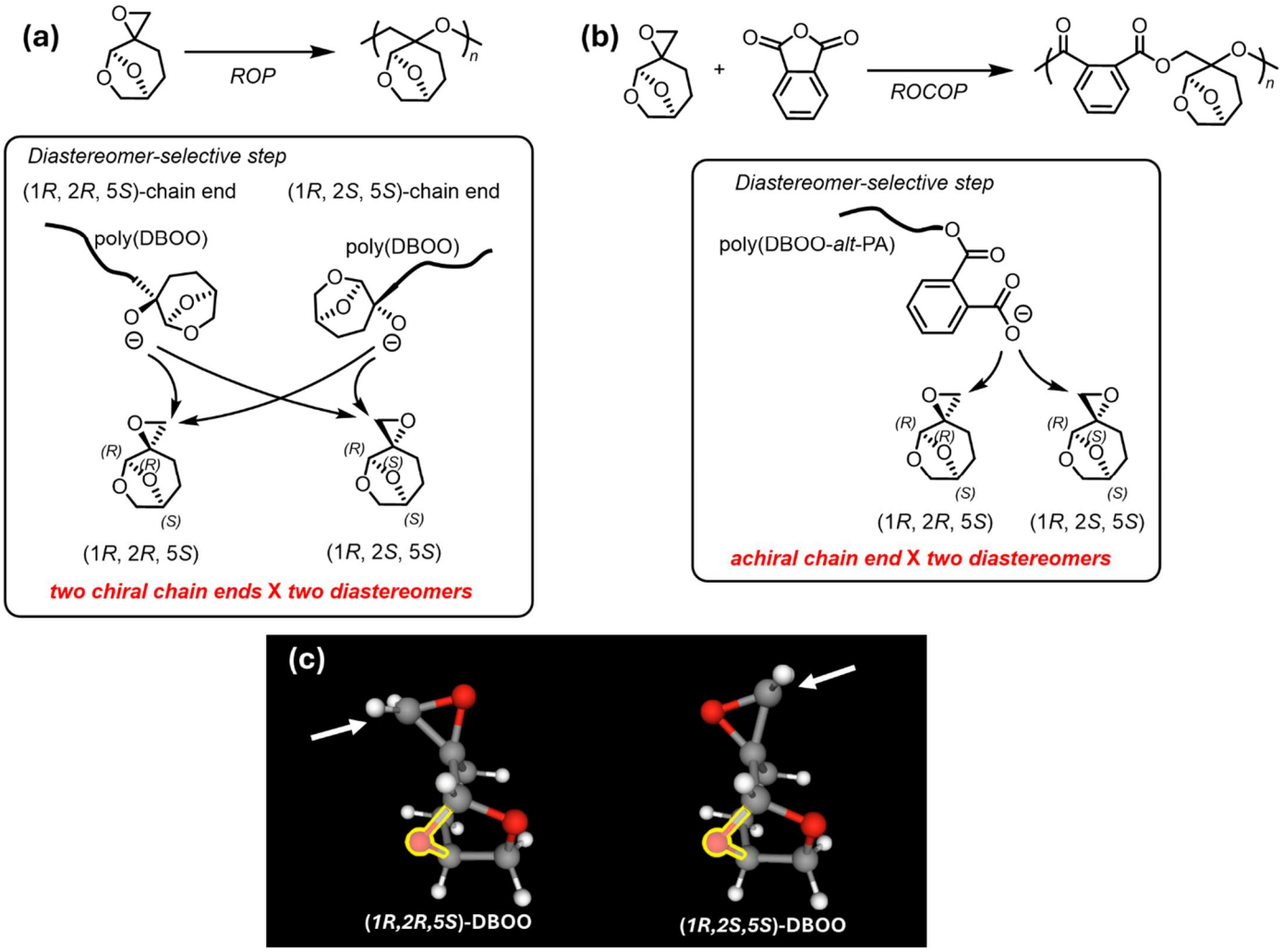

Figure S7. Comparison of ^{1}H NMR spectra of poly(DBOO$_{(50:50)}$-*alt*-PA) (down) and poly(DBOO$_{(87:13)}$-*alt*-PA) (upper)

Note: In the ROP of DBOO, (1*R*, 2*S*, 5*S*)-diastereomer was consumed approximately 1.6 times faster than the (1*R*, 2*R*, 5*S*)-diastereomer. In contrast, in the present ROCOP of PA and DBOO, the difference in the reaction rates of the two DBOO diastereomers was much smaller (**Table S1 and Figure 2D**). We believe that this difference can be rationalized by considering their respective reaction mechanisms (**Figure S7**).

In the ROP of DBOO, two different types of alkoxide chair chain ends are generated during propagation (**Figure S7a**). As a result, four distinct propagation pathways are possible, making the overall stereochemical preference difficult to interpret intuitively.

In contrast, in the ROCOP system, the diastereomer-selective step is the ring opening of the DBOO epoxide via nucleophilic attack by the carboxylate chain end (**Figure S7b**). Because the propagating carboxylate chain end can reasonably be regarded as effectively achiral, as the chiral DBOO unit is spatially distant from the reactive site, the stereochemical analysis can be simplified to considering only the 3D structures of the two DBOO diastereomers themselves. As shown in **Figure S7c**, the steric environments around the epoxide moieties of the two diastereomers are not significantly different. This observation is consistent with the much smaller difference in the consumption rates of the two DBOO diastereomers during ROCOP with PA.

poly(DBOO$_{(50:50)}$-*alt*-GA)

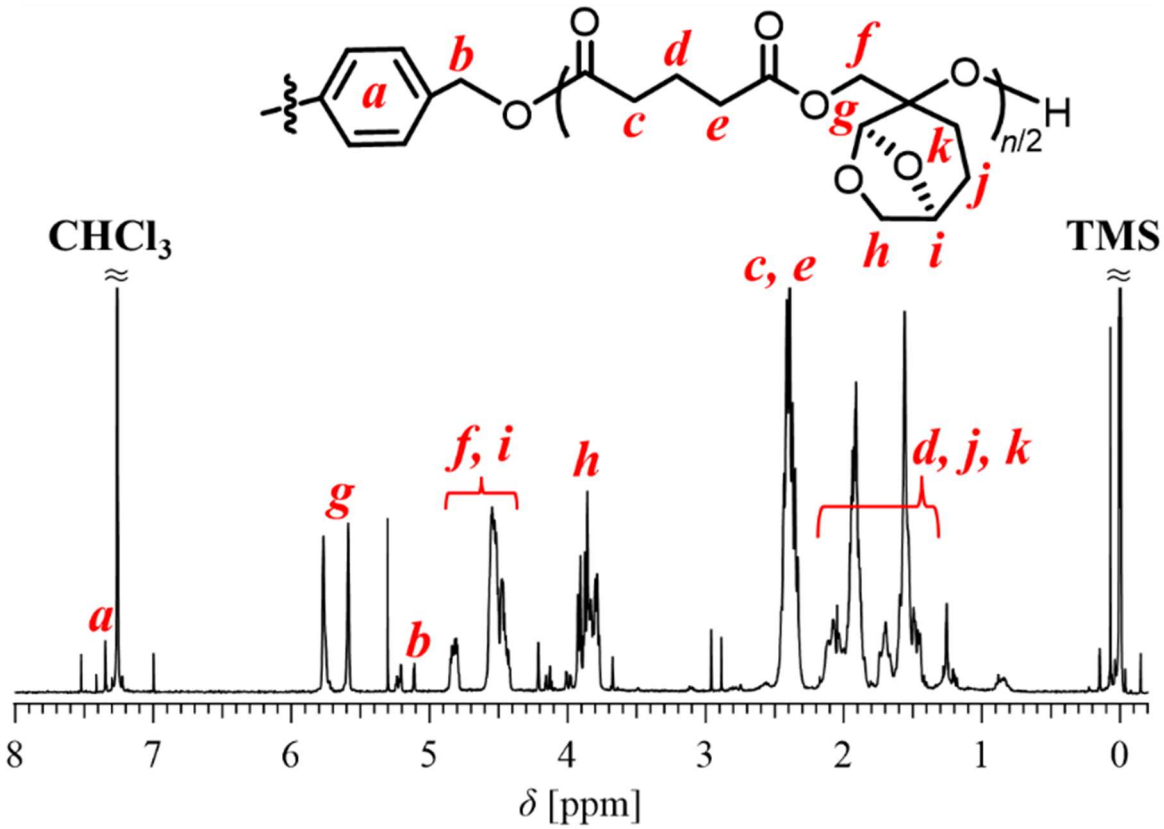

Figure S8. ^{1}H NMR spectrum of poly(DBOO$_{(50:50)}$-*alt*-GA) (Table 2, run 1; 400 MHz, $CDCl_3$).

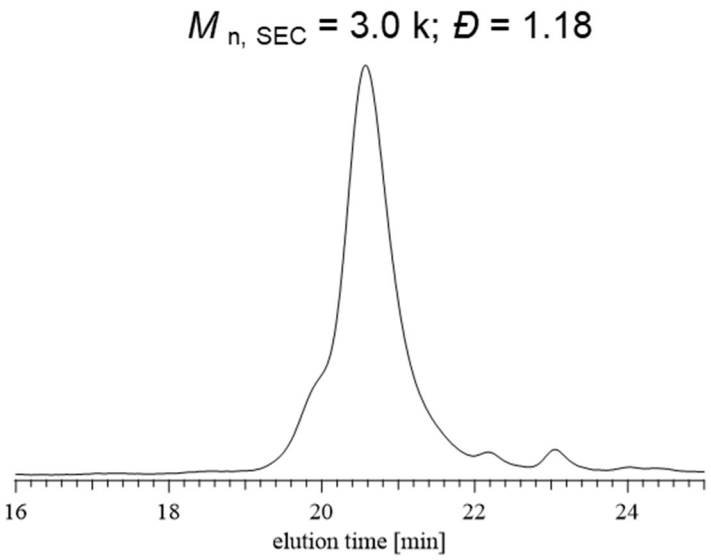

Figure S9. SEC trace of poly(DBOO$_{(50:50)}$-*alt*-GA) (Table 2, run 1).

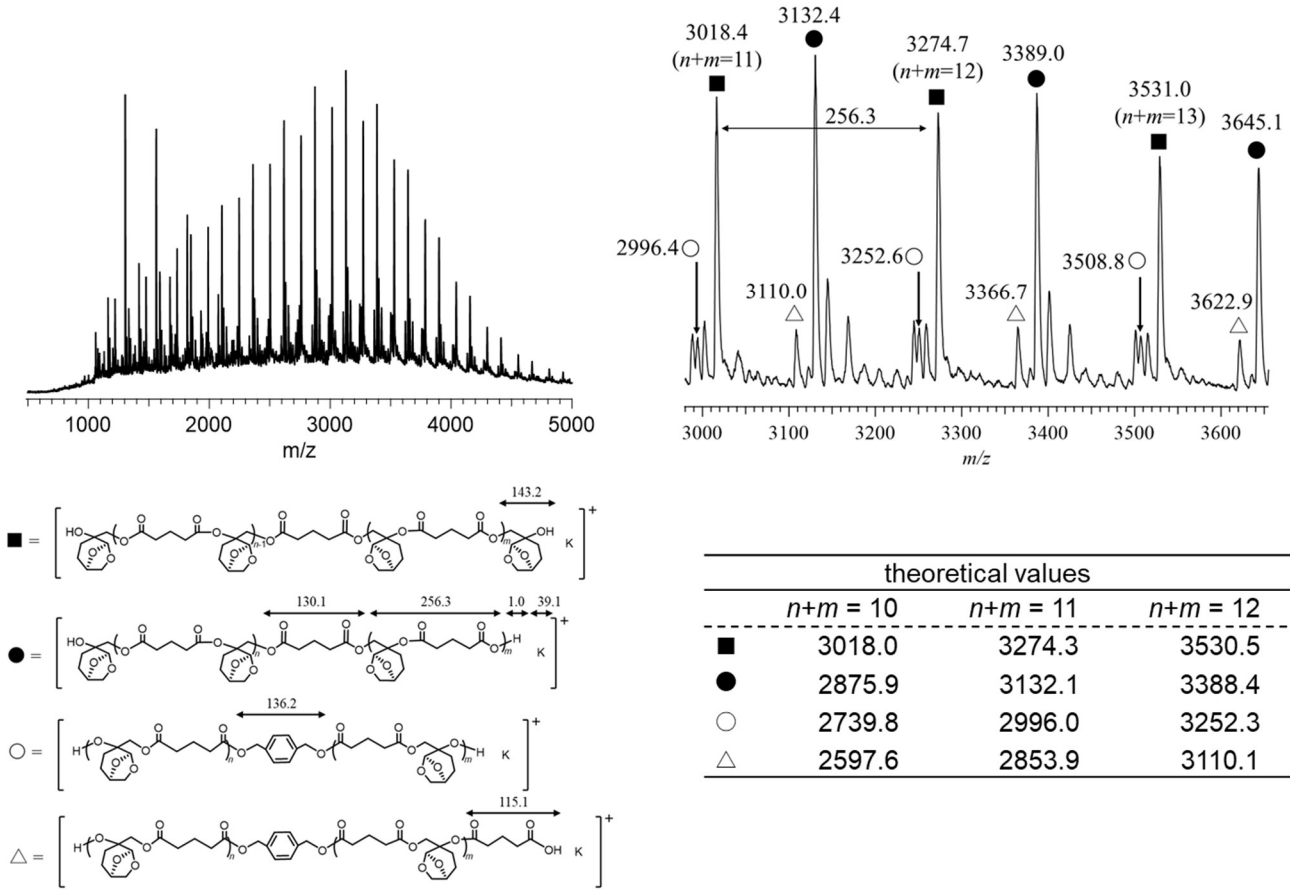

theoretical values			
	n+*m* = 10	*n*+*m* = 11	*n*+*m* = 12
■	3018.0	3274.3	3530.5
●	2875.9	3132.1	3388.4
○	2739.8	2996.0	3252.3
△	2597.6	2853.9	3110.1

Figure S10. MALDI-TOF MS of poly(DBOO$_{(50:50)}$-*alt*-GA) (Table 2, run 1).

poly(DBOO$_{(50:50)}$-*alt*-DGA)

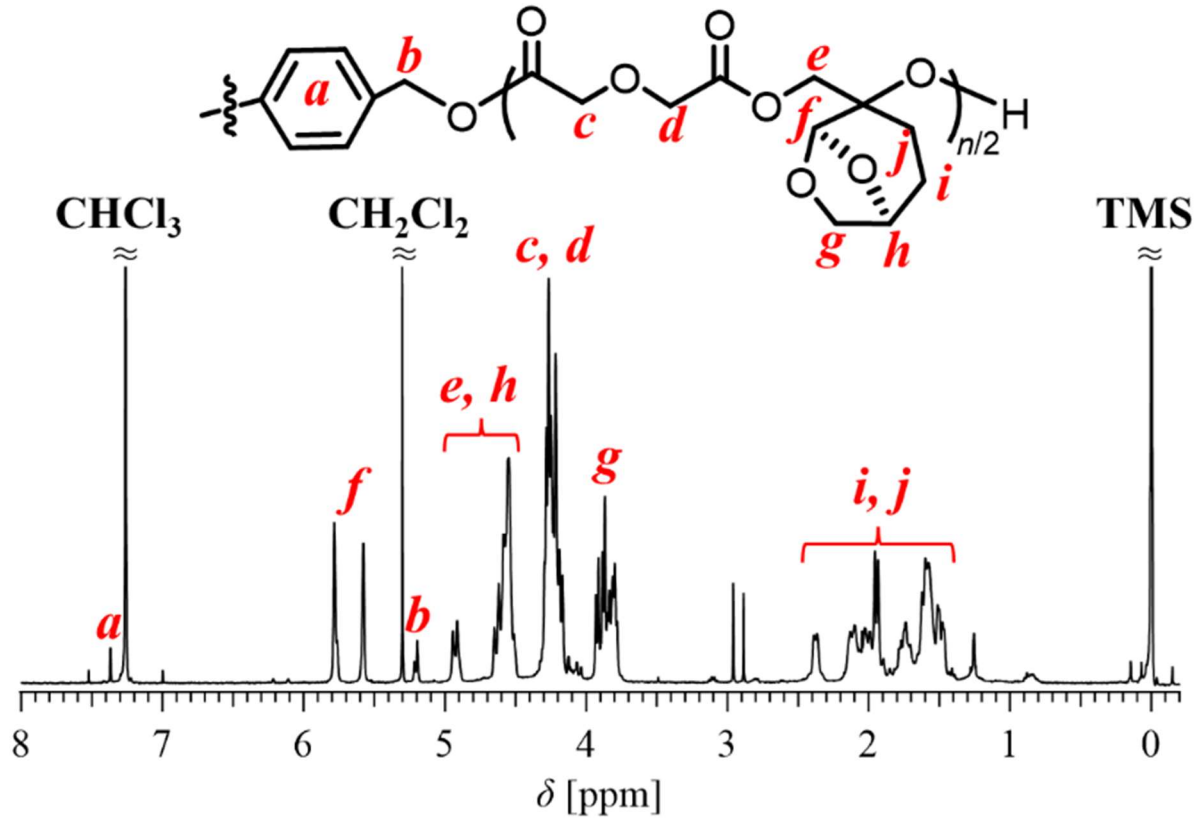

Figure S11. ^{1}H NMR spectrum of poly(DBOO$_{(50:50)}$-*alt*-DGA) (Table 2, run 2; 400 MHz, $CDCl_3$).

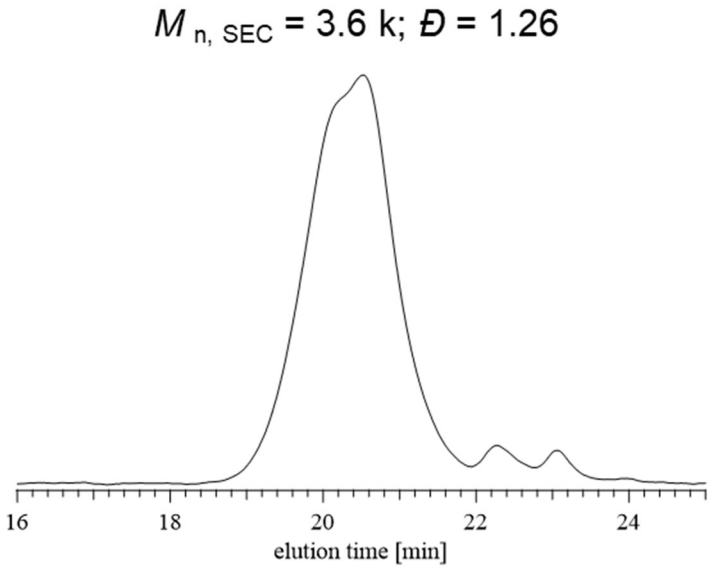

Figure S12. SEC trace of poly(DBOO$_{(50:50)}$-*alt*-DGA) (Table 2, run 2).

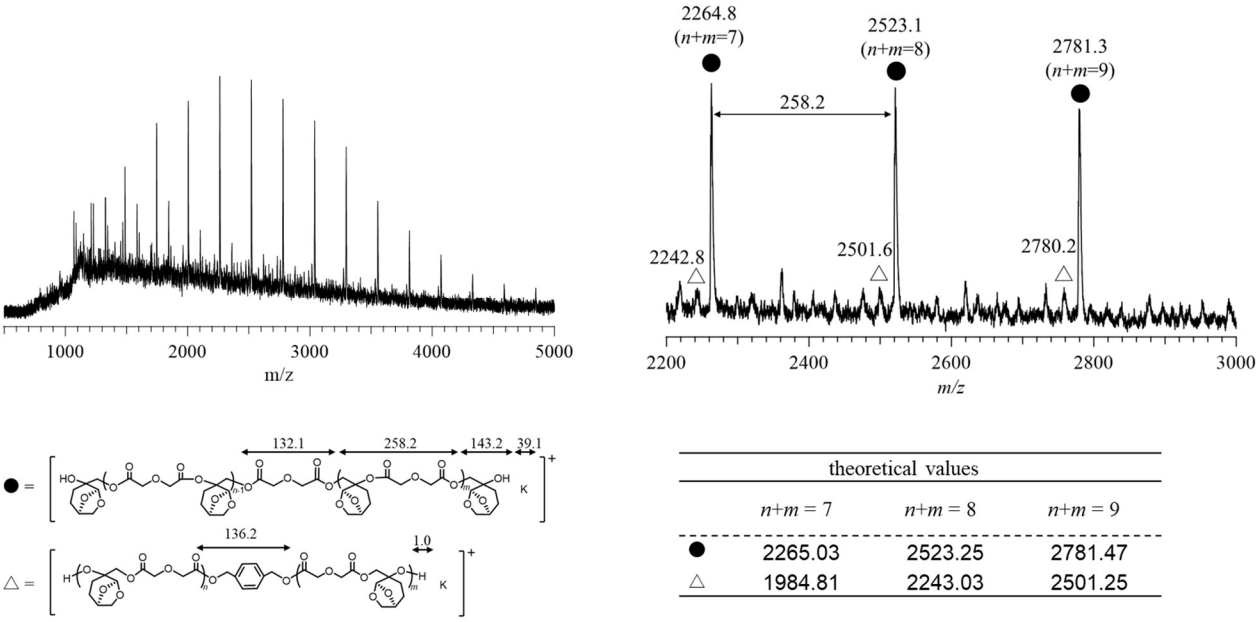

	theoretical values		
	$n+m = 7$	$n+m = 8$	$n+m = 9$
●	2265.03	2523.25	2781.47
△	1984.81	2243.03	2501.25

Figure S13. MALDI-TOF MS of poly(DBOO$_{(50:50)}$-*alt*-DGA) (Table 2, run 2).

poly(DBOO$_{(50:50)}$-*alt*-NA)

Table S2. Some initial attempts in ROCOP of DBOO$_{(50:50)}$ and NA.

Run	[NA]$_0$/[DBOO]$_0$/[I]$_0$/[CsOPiv.]	Temp. (°C)	Time (h)	Conv.$_{PA}$ (%)	$M_{n,theo.}$	$M_{n,NMR}$	$M_{n,SEC}$ [b]	$Đ$ [b]
1	77/70/1/1	100	72	n.d.	n.d.	n.d.	1,700	1.74
2	77/70/1/1	80	158	n.d.	n.d.	n.d.	1,400	1.48

[a] Polymerization conditions: Ar atmosphere; BDM for initiator. [b] Determined by SEC measurement of the obtained polymer in THF using polystyrene standard.

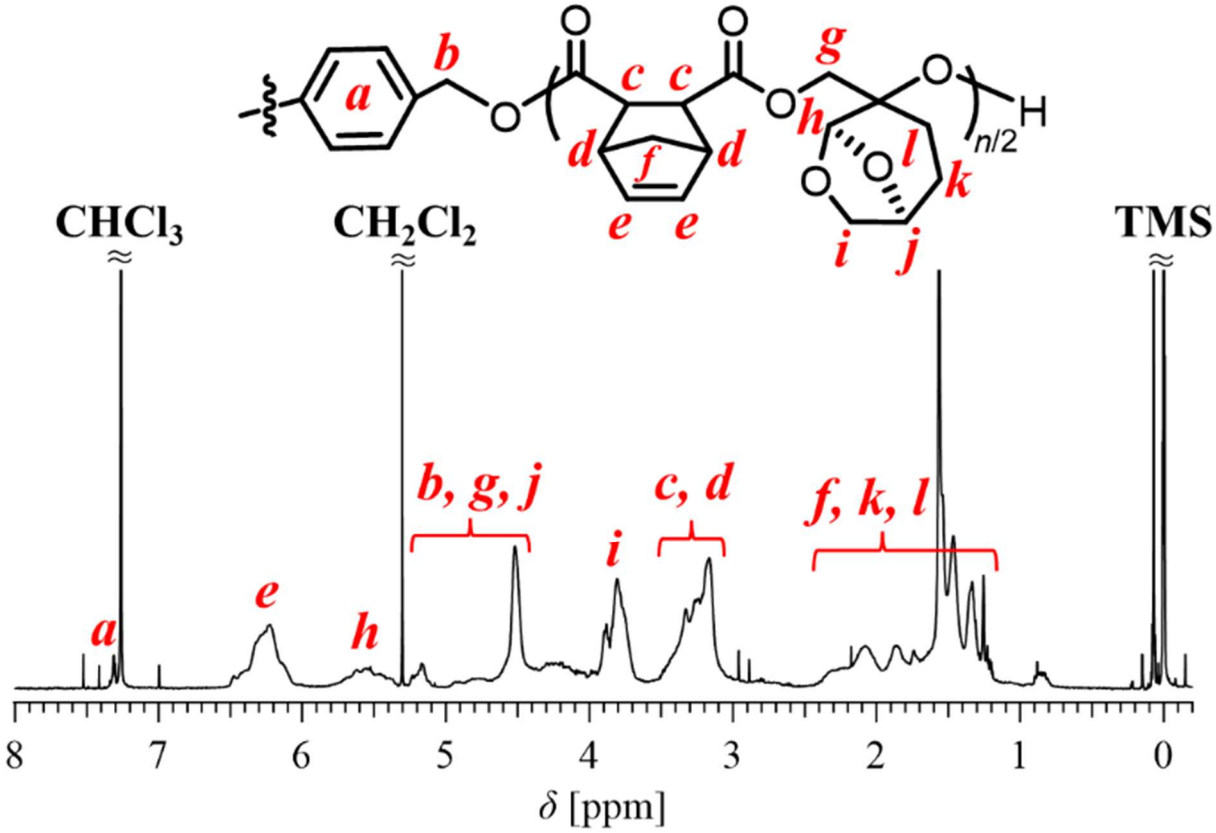

Figure S14. ^{1}H NMR spectrum of poly(DBOO$_{(50:50)}$-*alt*-NA) (Table 2, run 3; 400 MHz, $CDCl_3$).

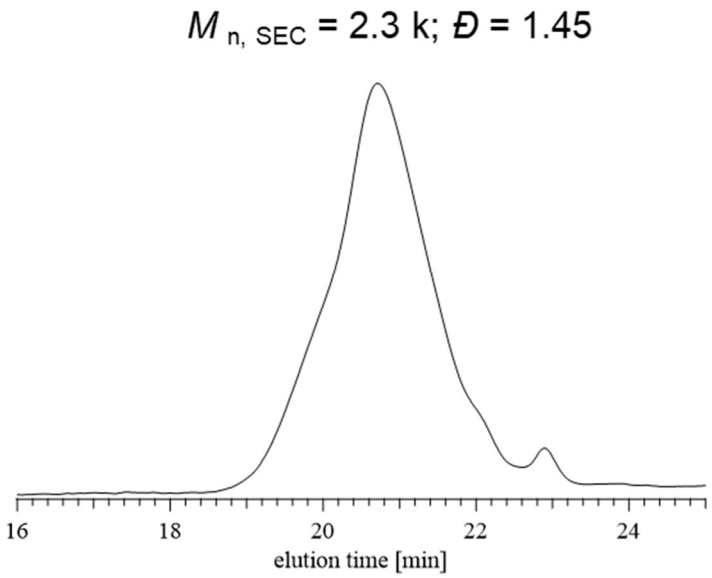

Figure S15. SEC trace of poly(DBOO$_{(50:50)}$-*alt*-NA) (Table 2, run 3).

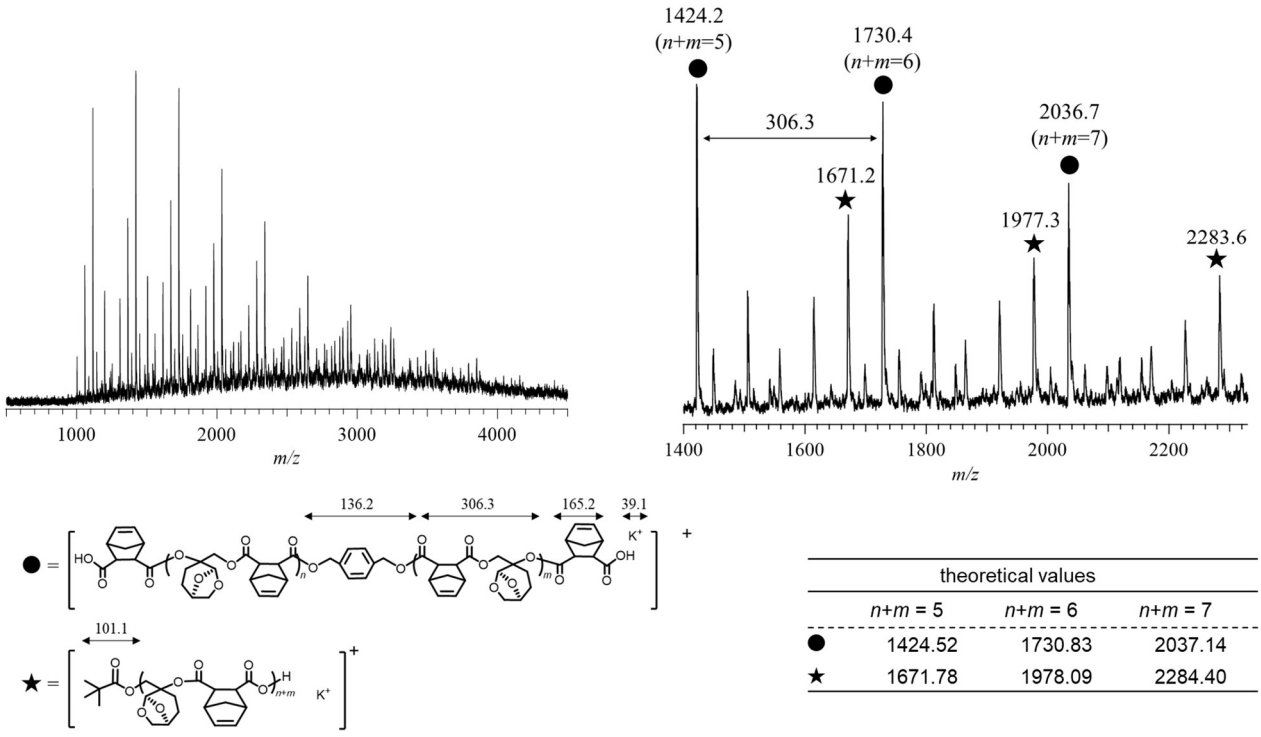

theoretical values			
	n+*m* = 5	*n*+*m* = 6	*n*+*m* = 7
●	1424.52	1730.83	2037.14
★	1671.78	1978.09	2284.40

Figure S16. MALDI-TOF MS of poly(DBOO$_{(50:50)}$-*alt*-NA) (Table 2, run 3).

DBOOPh

Synthetic details

Aryl functionalization of levoglucosenone (LGO) via 1, 4-addition reaction

Scheme S2. Synthesis of LGOPh

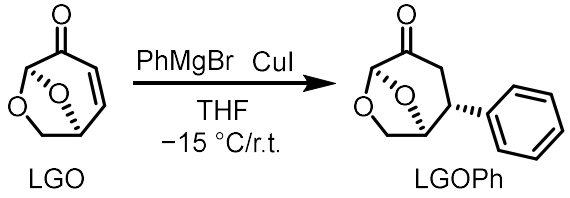

Copper(I) iodide (758 mg, 4.0 mmol, 1.0 eq.) was placed in a flask, and the system was purged with argon. Dry THF (15 mL) was added under an argon atmosphere, and the mixture was stirred and cooled to −15 °C. A solution of phenylmagnesium bromide (1.0 M in THF, 8.0 mL, 8.0 mmol, 2.0 eq.) was added dropwise at −15 °C. The reaction mixture was stirred for 10 min at −15 °C and then for an additional 20 min at room temperature. After cooling again to −15 °C, a mixed solution of LGO (508 mg, 4.0 mmol, 1.0 eq.) dissolved in dry THF (5 mL) was added. The reaction was maintained at −15 °C for 1.5 h and then quenched by the addition of 1 M aq. HCl (10 mL). The resulting mixture was filtered through Celite, and the filtrate was extracted with ethyl acetate (500 mL × 3). The combined organic layers were washed with saturated brine (300 mL), dried over anhydrous $MgSO_4$, filtered, and concentrated under reduced pressure. The crude residue was purified by silica gel column chromatography (hexane/ethyl acetate = 5/1 (v/v), R_f = 0.18) to afford LGOPh as a white solid (yield: 248 mg, 30.1%). The structure of the product was confirmed by comparison of its ^{1}H NMR and ^{13}C NMR spectra with the literature data[2].

Epoxidation of LGOPh via the corey-chaykovsky reaction

Scheme S3. Synthesis of DBOOPh

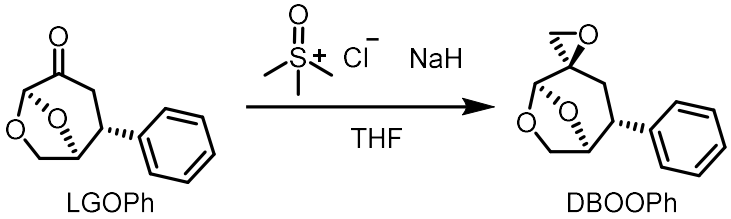

Trimethylsulfoxonium chloride (224 mg, 1.74 mmol, 1.8 eq.) and sodium hydride (201.3 mg of a 60% dispersion in paraffin liquid, 1.85 mmol, 1.9 eq.) were placed in a flask, and the system was purged with argon. Dry THF (40 mL) was added under an argon atmosphere, and the mixture was stirred and heated to 50 °C. After gas evolution had completely ceased, a mixed solution of LGOPh (201 mg, 0.984 mmol, 1.0 eq.) dissolved in dry THF (20 mL) was added dropwise in an ice bath. The reaction mixture was stirred at room temperature for 5 h and then quenched by the addition of water (100 mL). The resulting mixture was extracted with ethyl acetate (100 mL × 5). The combined organic layers were washed with saturated brine (200 mL), dried over anhydrous $MgSO_4$, filtered, and concentrated under reduced pressure. The crude residue was purified by silica gel column chromatography (hexane/ethyl acetate = 5/1 (v/v), R_f = 0.13) to afford DBOOPh as a white solid (yield: 159 mg, 74.1%).

^{1}H NMR (400 MHz, $CDCl_3$): δ (ppm) 7.56-7.24 (m, 5H, -C_6H_5), 4.86 (s, 1H, -OC*H*O-), 4.64 (d, J = 4.1 Hz, 1H, -OCH_2C*H*O-), 4.10-3.97 (m, 2H, -OCH_2CHO-), 3.03 (d, J = 7.7 Hz, 1H, -C*H*C_6H_5), 2.88 (dd, J = 16, 8.4 Hz, 1H, -CHCH_2C-), 2.85 (d, J = 4 Hz, 1H, -CCH_2O-), 2.71 (d, J = 4 Hz, 1H, -CCH_2O-), 1.59 (d, J = 14.8 Hz, 1H, -CHCH_2C-)

^{13}C NMR (100 MHz, $CDCl_3$): δ (ppm) 142.9 (-OCH*C*HC_6H_5), 128.7, 128.4, 126.8 (-OCHCHC_5H_5-), 104.4 (-O*C*HO-), 77.8(-OCH_2*C*HO-), 68.4 (-O*C*H_2CHO-), 55.3 (-*C*CH_2O-), 50.7 (-C*C*H_2O-), 43.4 (-*C*HCH$_2$CO-), 27.7 (-CH*C*H_2CO-)

HRMS: $[C_{13}H_{14}O_3Na]^+$, m/z 241.08352. (Theoretical value: 241.08352) (**Figure S20**)

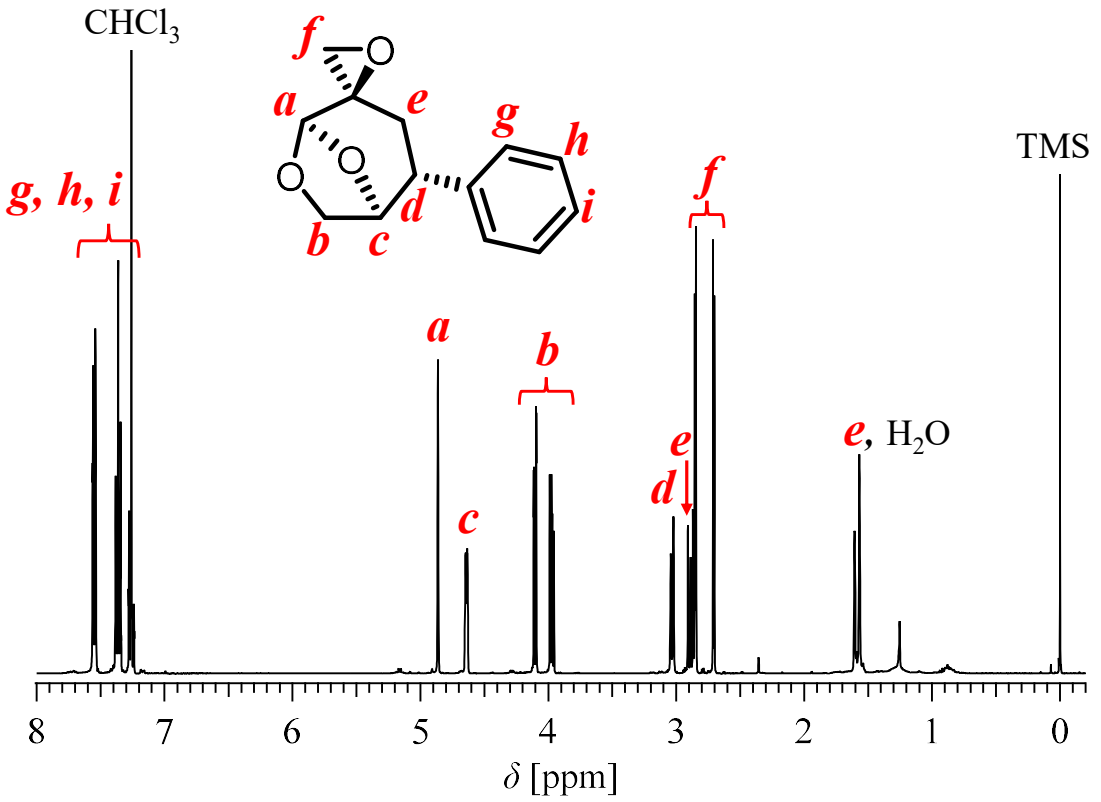

Figure S17. ^{1}H NMR spectrum of DBOOPh.

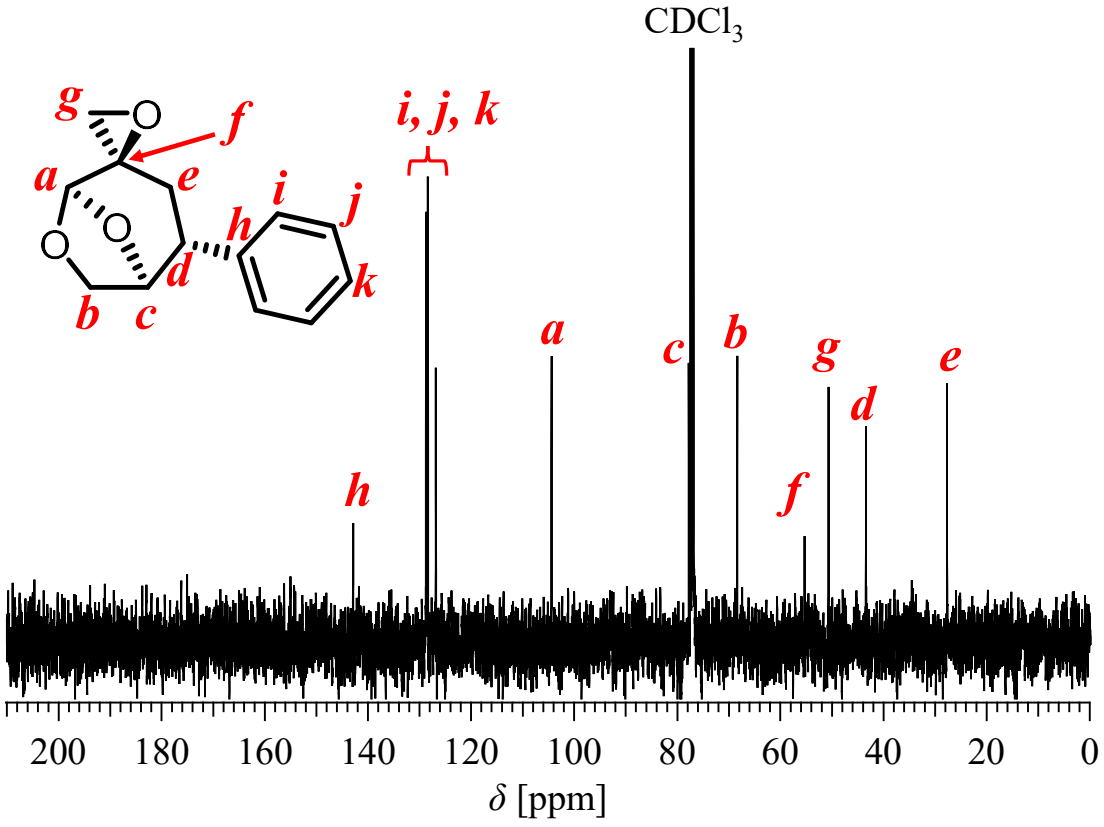

Figure S18. ^{13}C NMR spectrum of DBOOPh.

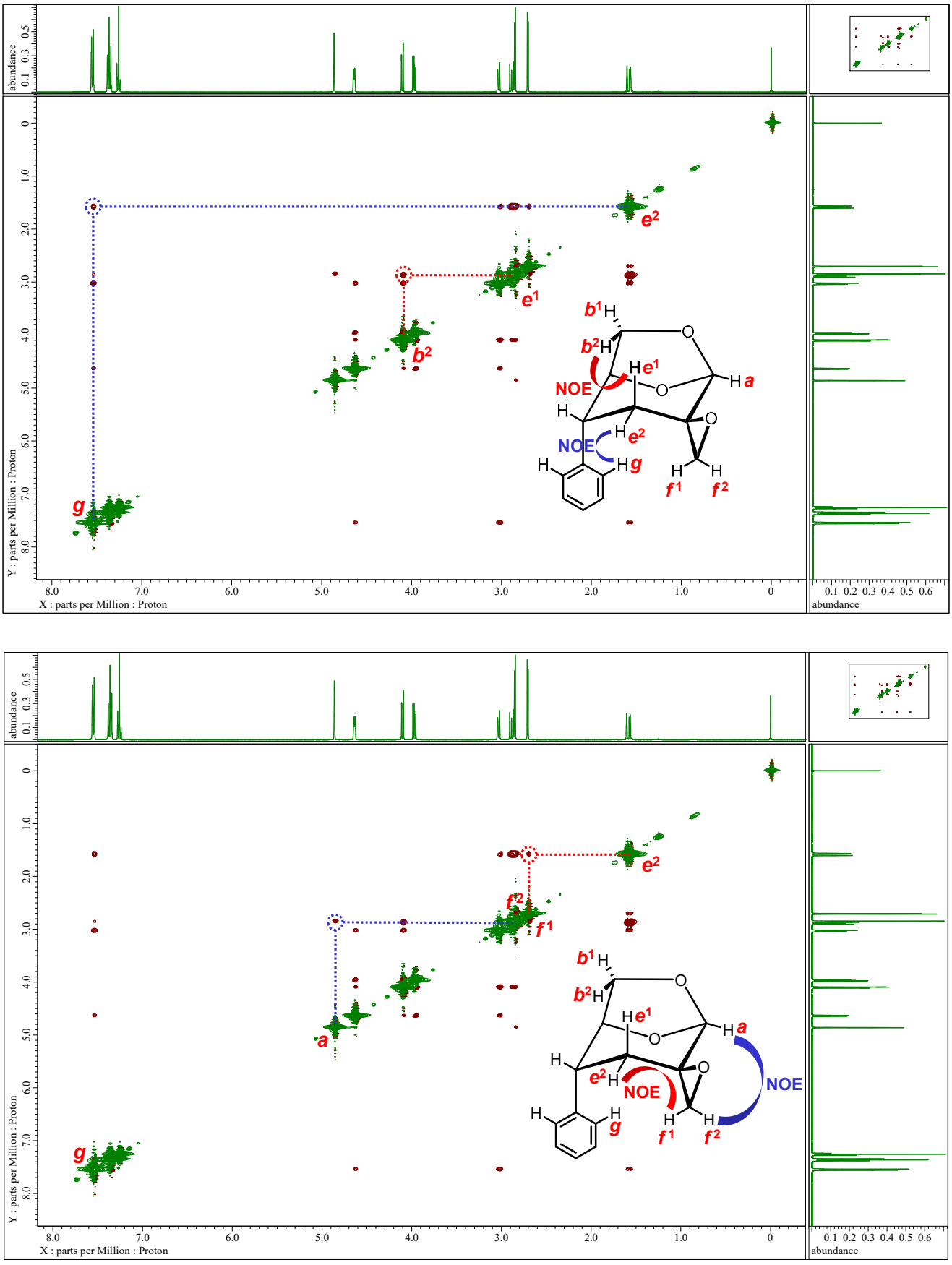

Figure S19. NOESY NMR spectrum of DBOOPh.

(a)

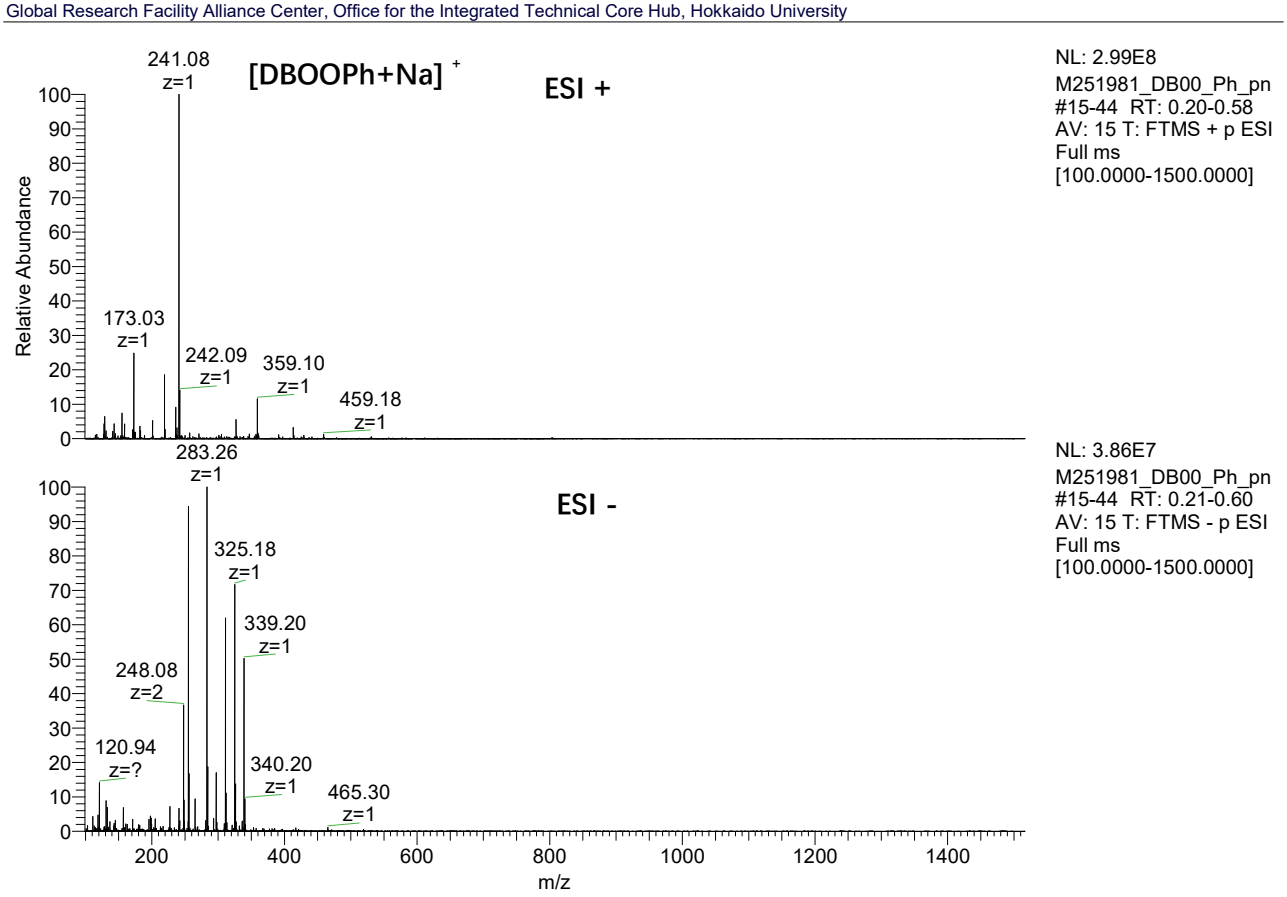

(b)

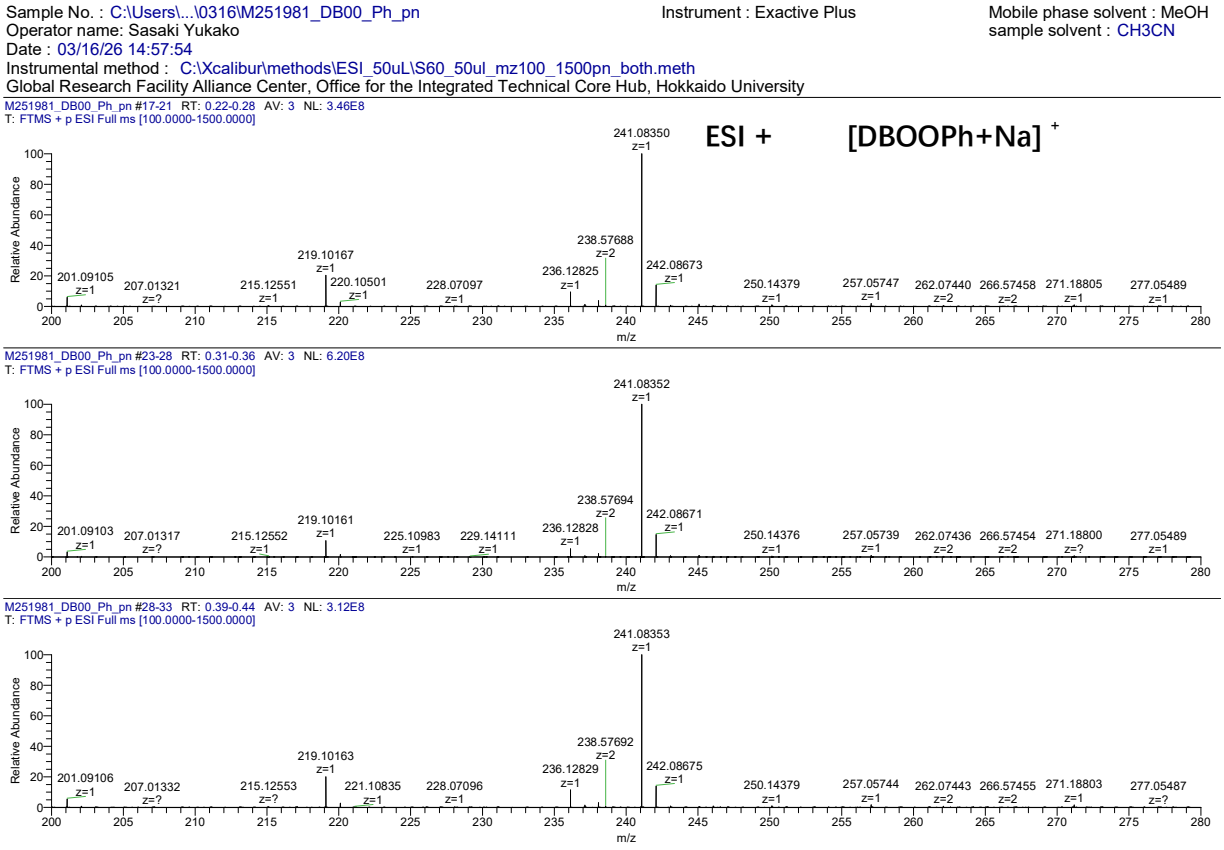

Figure S20. ESI mass spectrum of DBOOPh: (a) ESI+ and ESI- in full range; (b) zoomed in ESI+ spectrum

poly(DBOOPh-*alt*-PA)

Table S3. Some initial attempts in ROCOP of DBOOPh and PA.

Run	$[PA]_0/[DBOOPh]_0/[I]_0/[CsOPiv.]$	Temp. (°C)	Time (h)	$Conv._{PA}$ (%)	$M_{n,theo.}$	$M_{n,NMR}$	$M_{n,SEC}$ [b]	$Đ$ [b]
1	100/100/1/1	100	135	14	n.d.	n.d.	n.d.	n.d.

[a] Polymerization conditions: Ar atmosphere; BDM for initiator. [b] Determined by SEC measurement of the obtained polymer in THF using polystyrene standard.

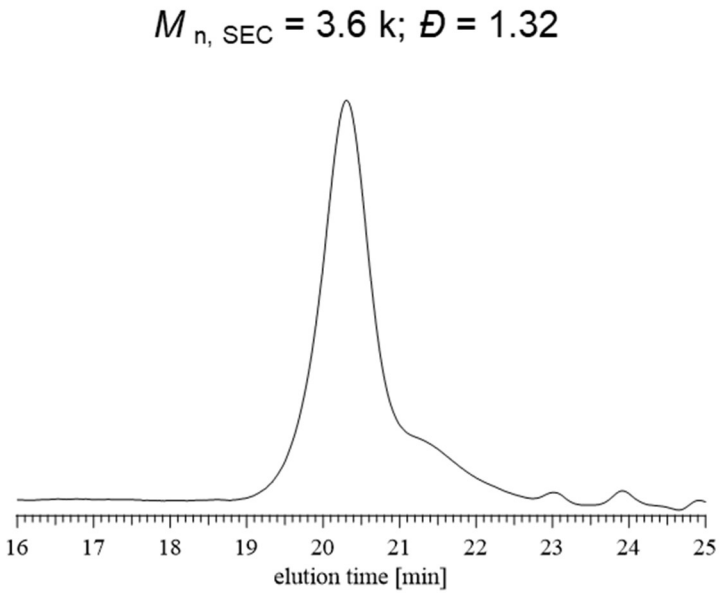

Figure S21. SEC trace of poly(DBOOPh-*alt*-PA) (Table 2, run 4).

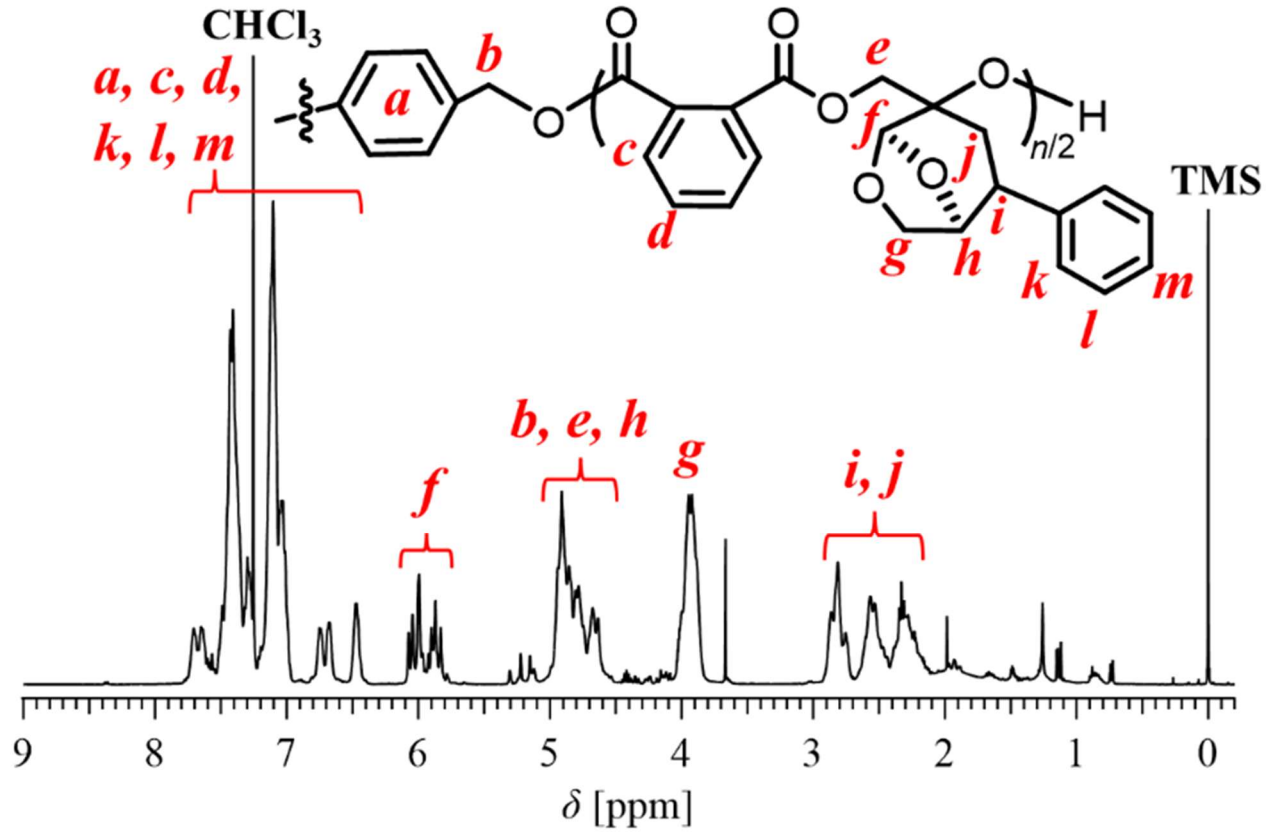

Figure S22. ^{1}H NMR spectrum of poly(DBOOPh-*alt*-PA) (Table 2, run 4; 400 MHz, $CDCl_3$).

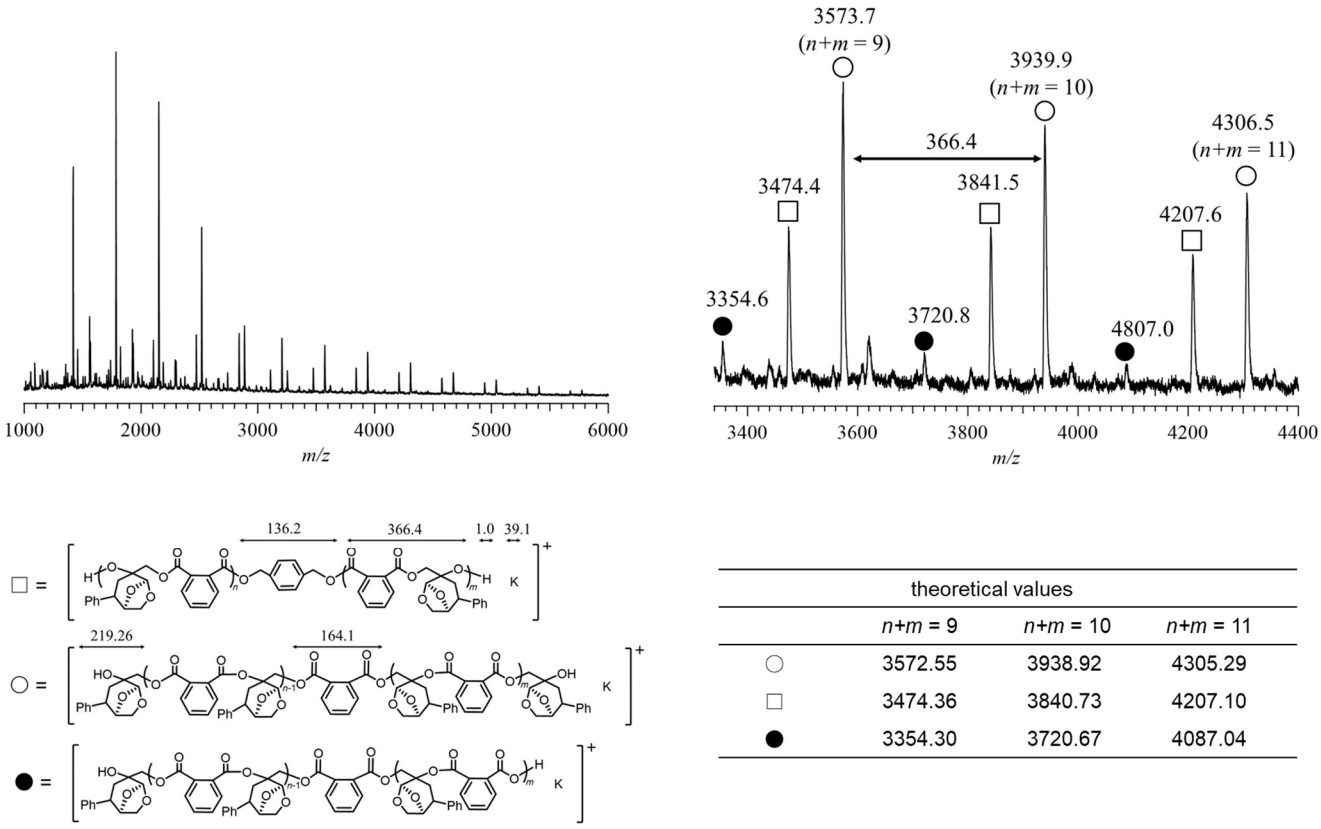

theoretical values			
	n+*m* = 9	*n*+*m* = 10	*n*+*m* = 11
○	3572.55	3938.92	4305.29
□	3474.36	3840.73	4207.10
●	3354.30	3720.67	4087.04

Figure S23. MALDI-TOF MS of poly(DBOOPh-*alt*-PA) (Table 2, run 4).

TGA

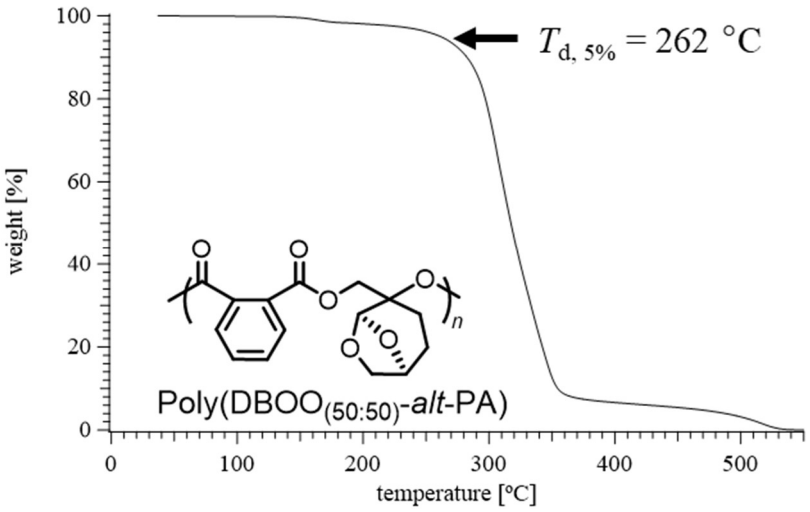

Figure S24. TGA traces of poly(DBOO$_{(50:50)}$-*alt*-PA) (Table 1, run 5).

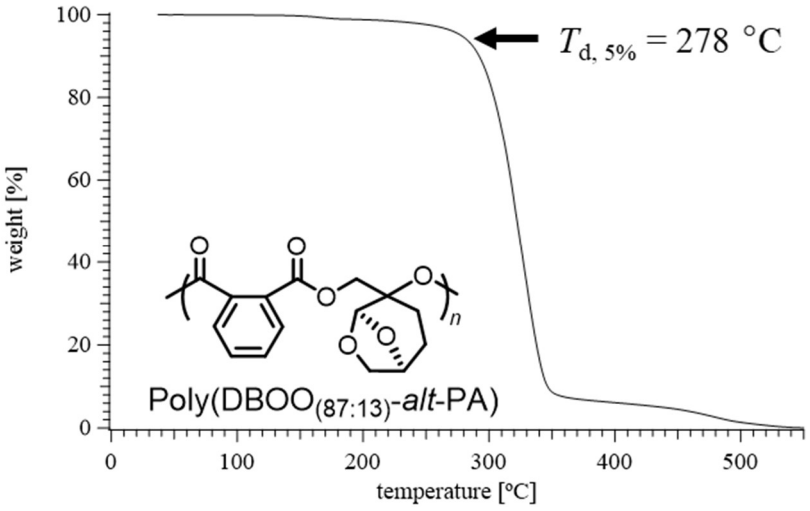

Figure S25. TGA traces of poly(DBOO$_{(87:13)}$-*alt*-PA) (Table 1, run 9).

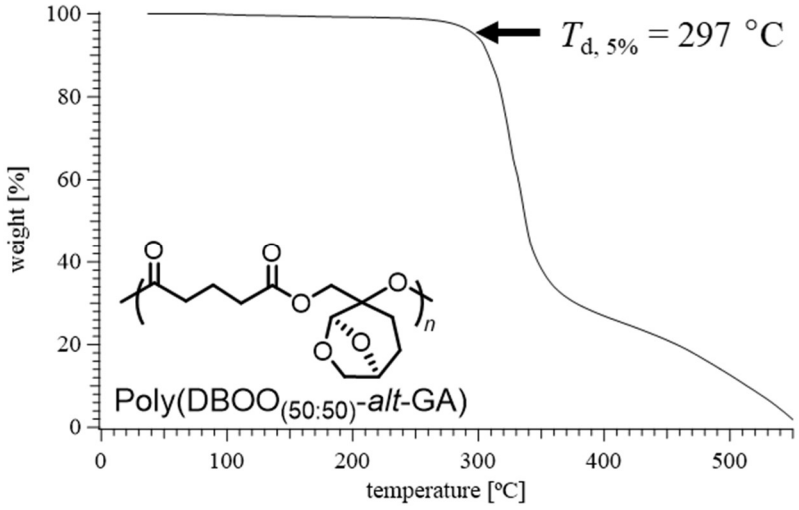

Figure S26. TGA traces of poly(DBOO$_{(50:50)}$-*alt*-GA) (Table 2, run 1).

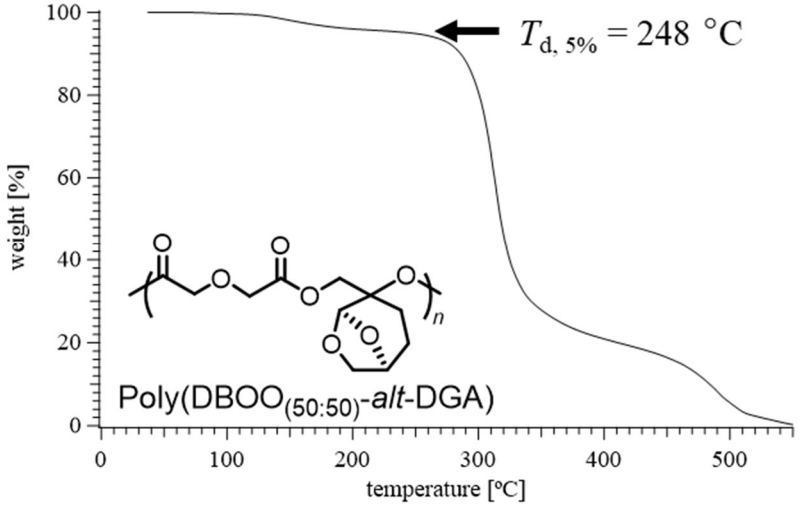

Figure S27. TGA traces of poly(DBOO$_{(50:50)}$-*alt*-DGA) (Table 2, run 2).

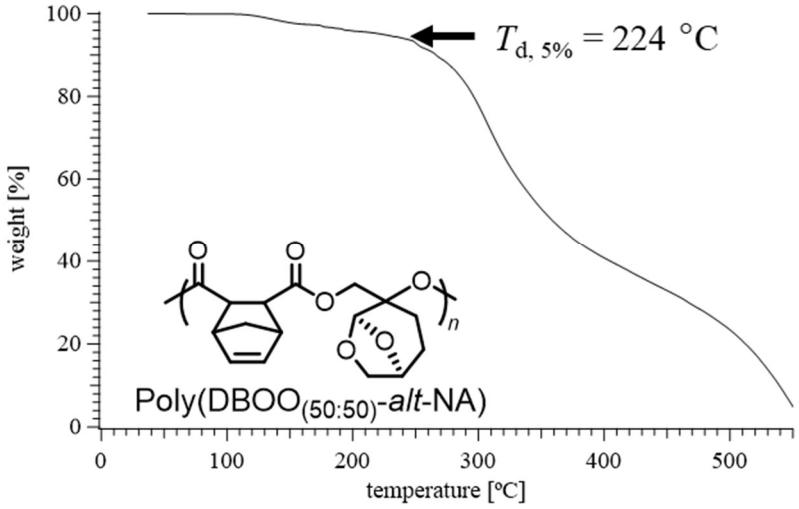

Figure S28. TGA traces of poly(DBOO$_{(50:50)}$-*alt*-NA) (Table 2, run 3).

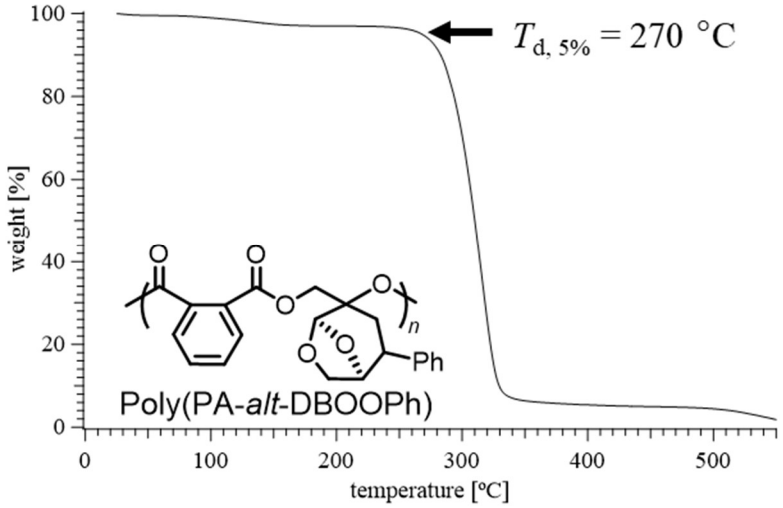

Figure S29. TGA traces of poly(DBOOPh-*alt*-PA) (Table 2, run 4).

DSC

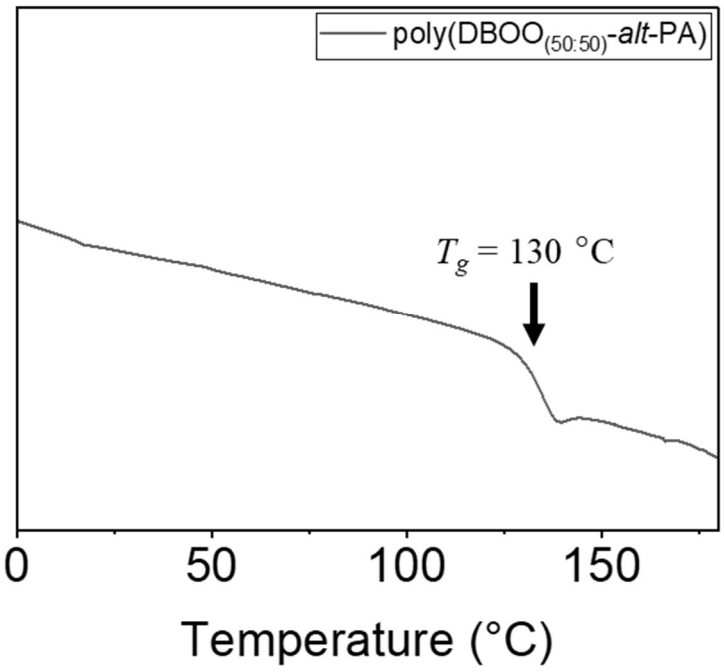

Figure S30. DSC traces of poly(DBOO$_{(50:50)}$-*alt*-PA) (Table 1, run 5).

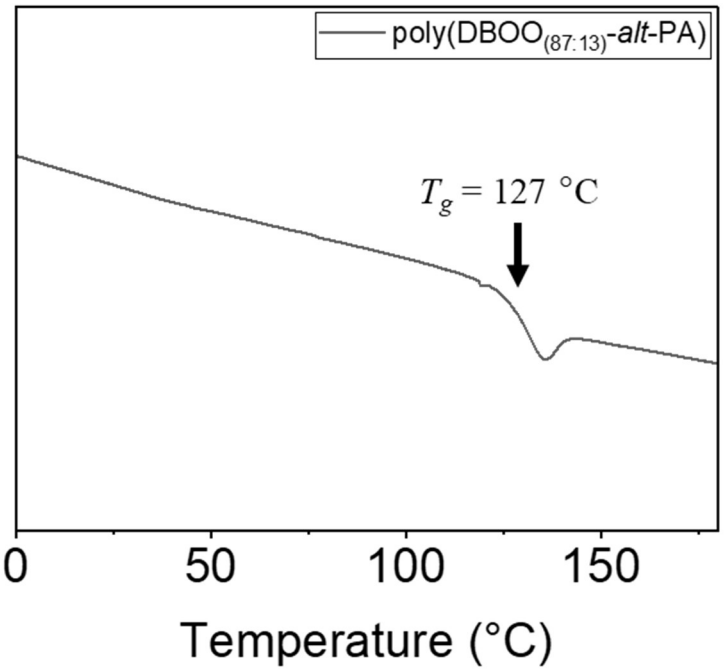

Figure S31. DSC traces of poly(DBOO$_{(87:13)}$-*alt*-PA) (Table 1, run 9).

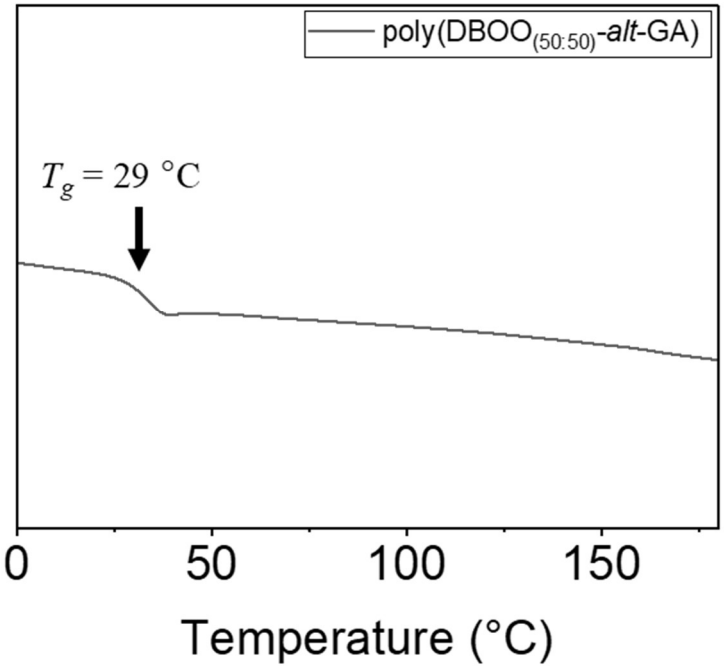

Figure S32. DSC traces of poly(DBOO$_{(50:50)}$-*alt*-GA) (Table 2, run 1).

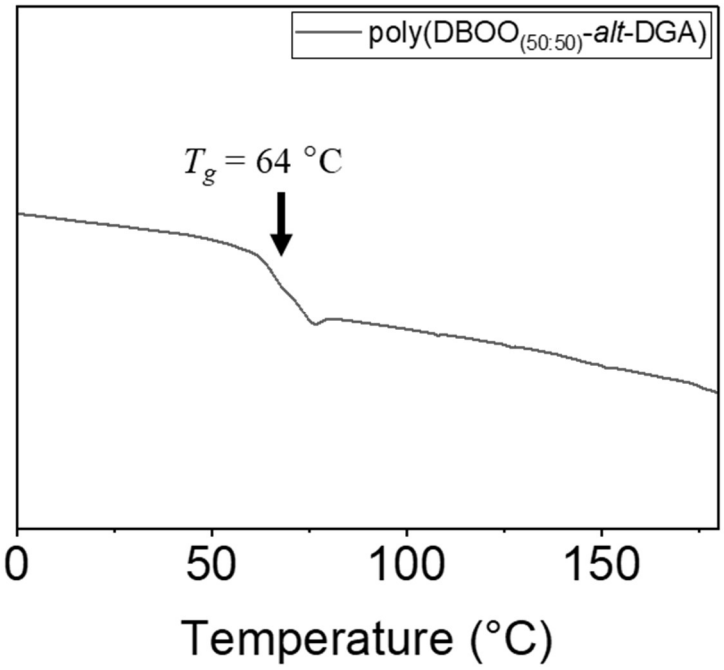

Figure S33. DSC traces of poly(DBOO$_{(50:50)}$-*alt*-DGA) (Table 2, run 2).

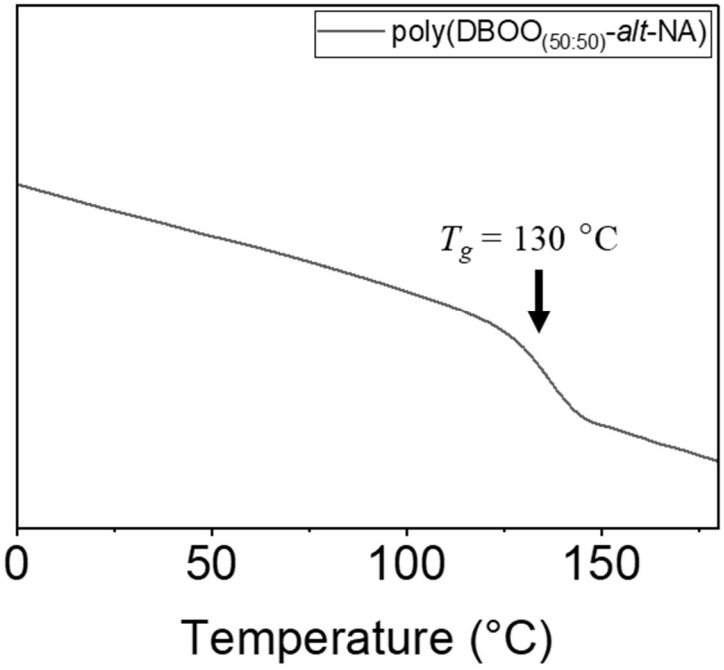

Figure S34. DSC traces of poly(DBOO$_{(50:50)}$-*alt*-NA) (Table 2, run 3).

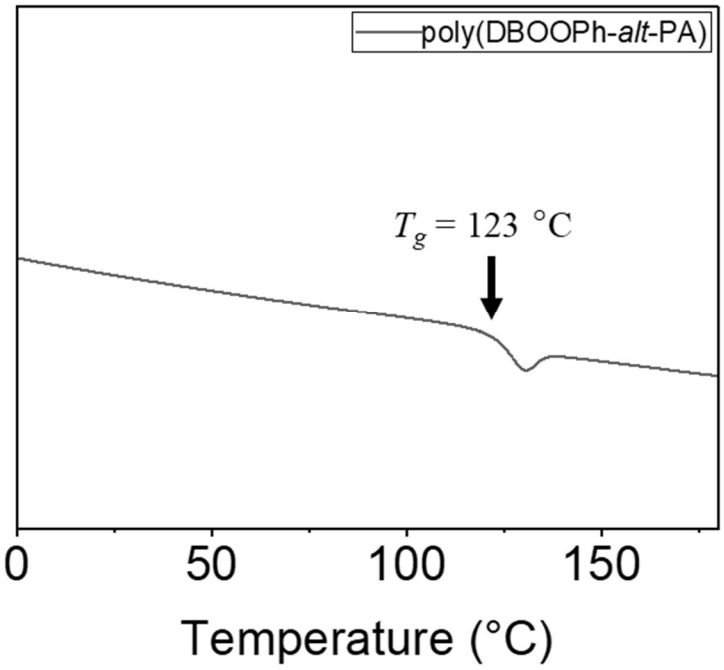

Figure S35. DSC traces of poly(DBOOPh-*alt*-PA) (Table 2, run 4).

PXRD

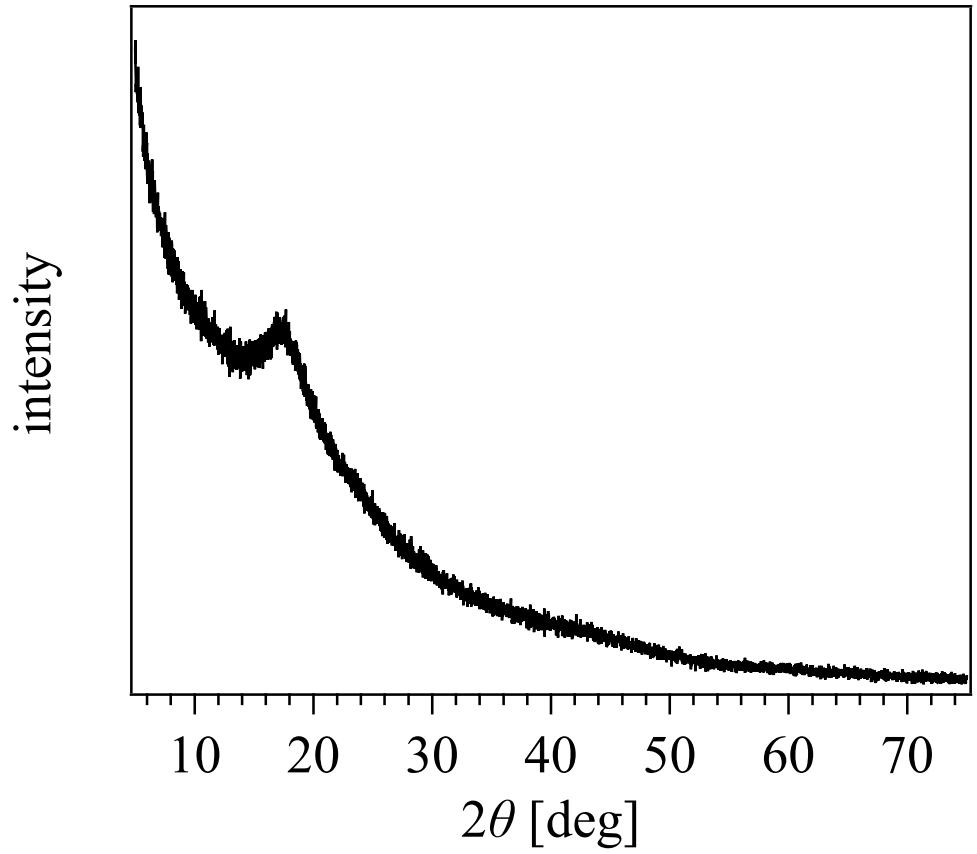

Figure S36. XRD traces of poly($DBOO_{(50:50)}$-*alt*-PA) (Table 1, run 5).

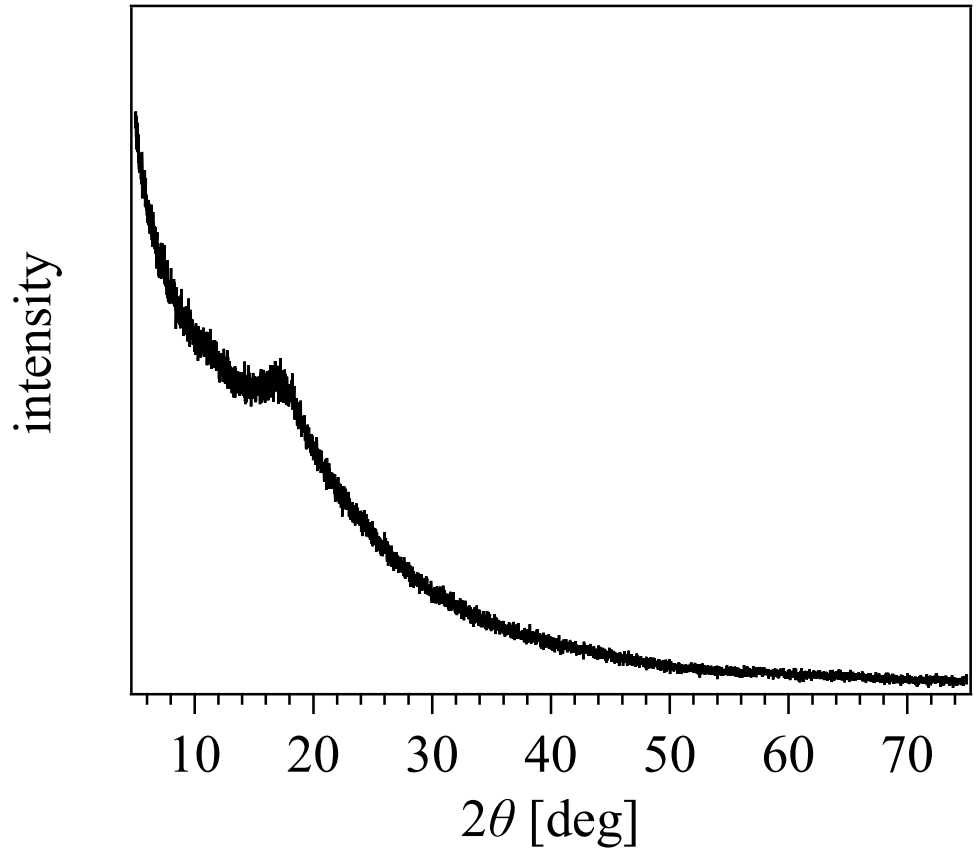

Figure S37. XRD traces of poly($DBOO_{(87:13)}$-*alt*-PA) (Table 1, run 9).

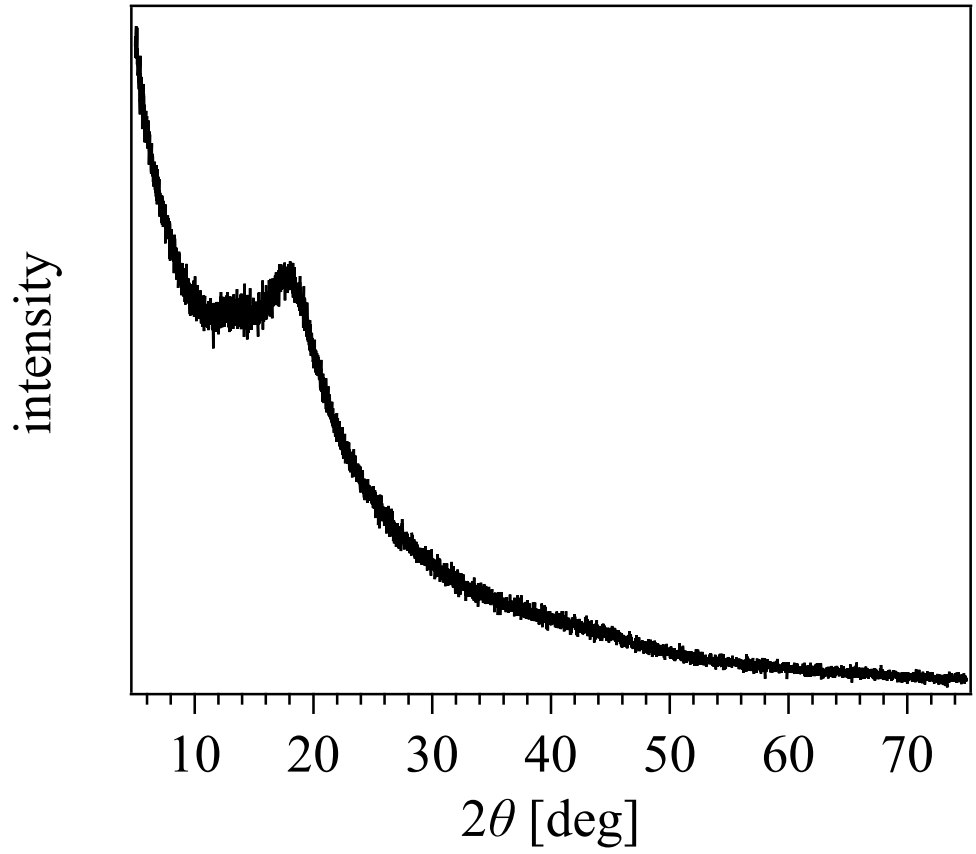

Figure S38. XRD traces of poly(DBOO$_{(50:50)}$-*alt*-GA) (Table 2, run 1).

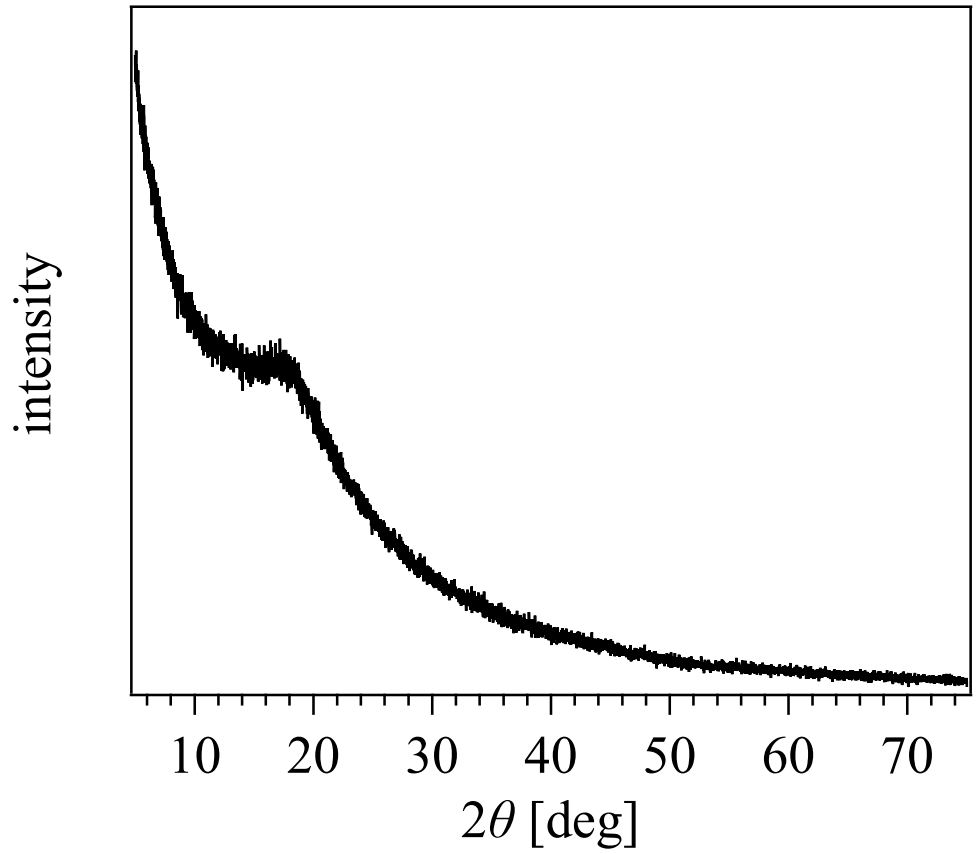

Figure S39. XRD traces of poly(DBOO$_{(50:50)}$-*alt*-DGA) (Table 2, run 2).

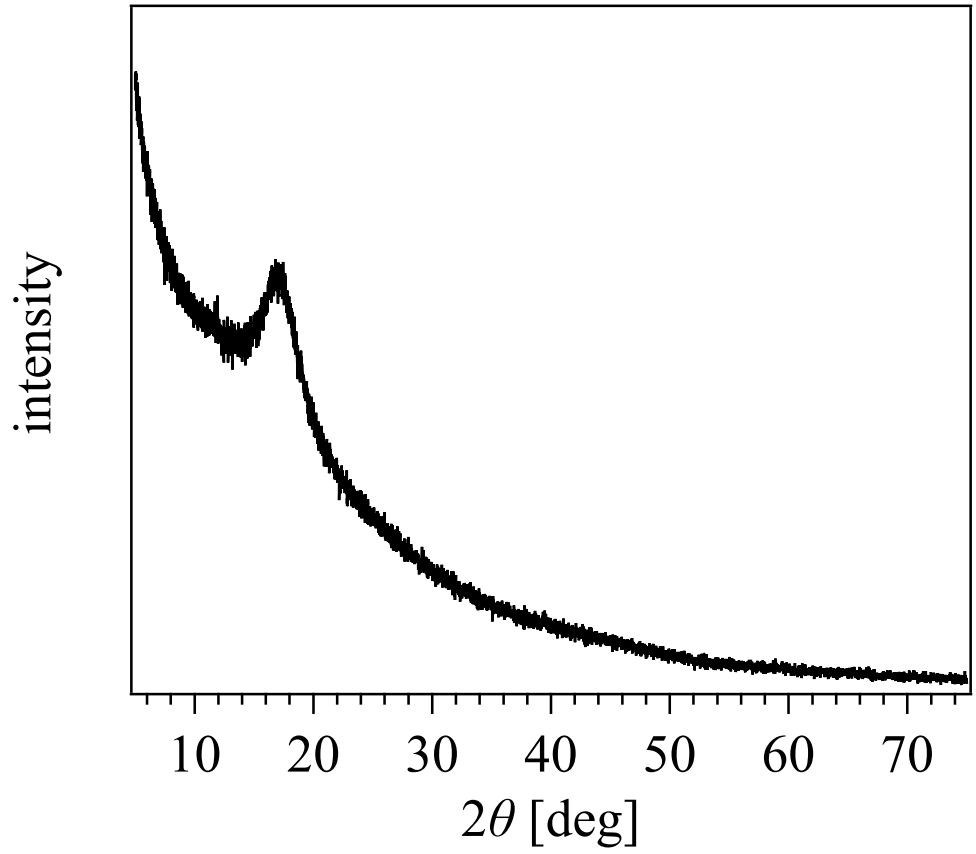

Figure S40. XRD traces of poly(DBOO$_{(50:50)}$-*alt*-NA) (Table 2, run 3).

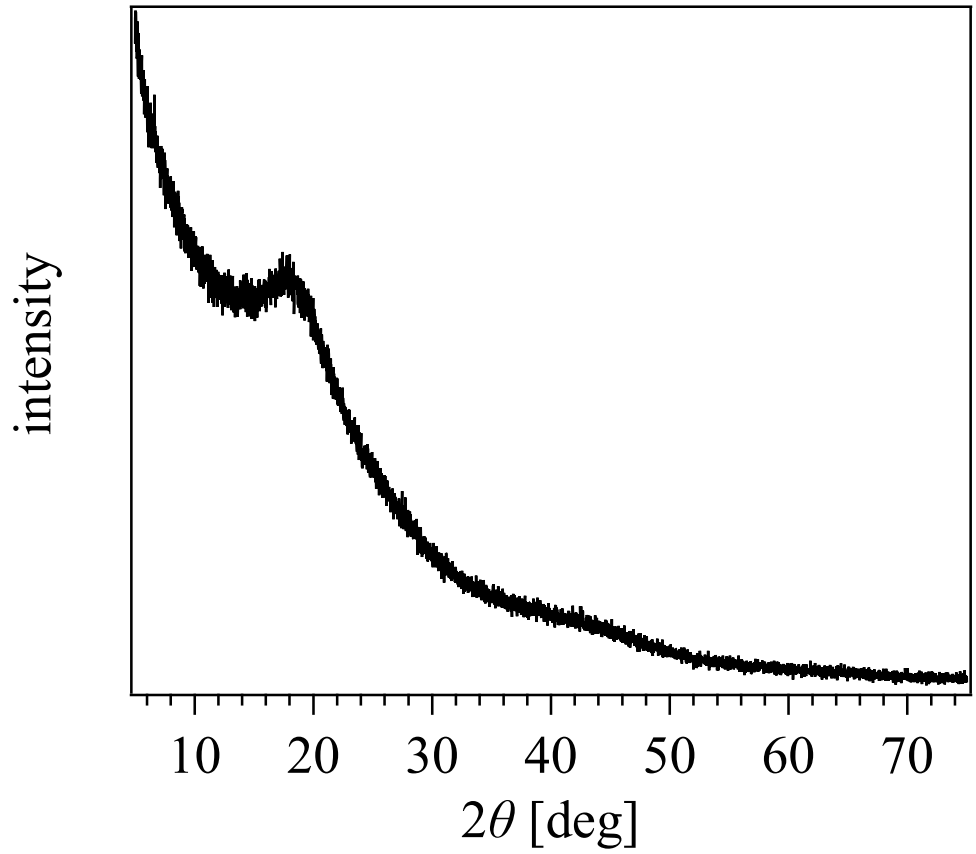

Figure S41. XRD traces of poly(DBOOPh-*alt*-PA) (Table 2, run 4).

CD

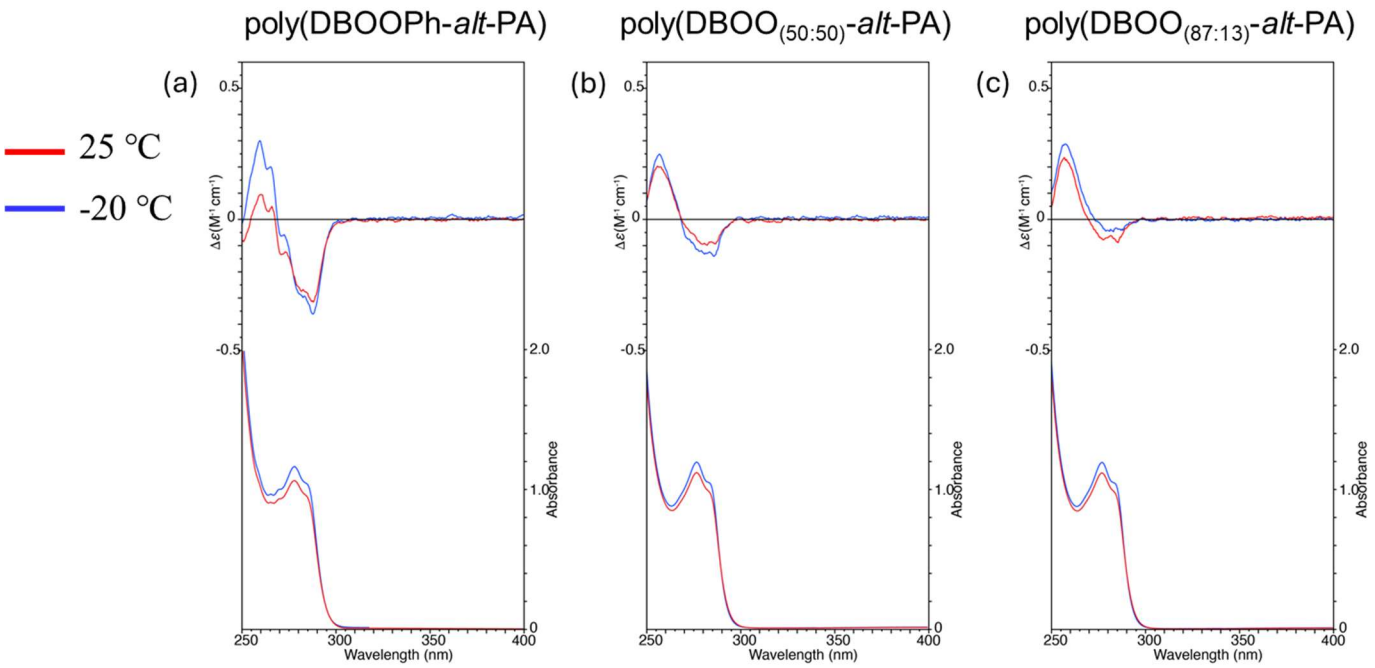

Figure S42. CD (top) and UV–vis absorption (bottom) spectra measured under 25 °C (red) and −20 °C (blue) at [polymer] = 10 mM (based on repeating units) in $CHCl_3$: (a) poly(DBOOPh-*alt*-PA); (b) poly($DBOO_{(50:50)}$-*alt*-PA); (c) poly($DBOO_{(87:13)}$-*alt*-PA)

Note: According to the CD spectra above, the CD signals were only slightly stronger at -20 °C than at 25 °C, indicating a weak temperature dependance of polymer conformation at this condition in $CHCl_3$.